The Mesoscale Structure of Severe Precipitation Systems in Switzerland

H. H. SCHIESSER

Atmospheric Science, Swiss Federal Institute of Technology, Zurich, Switzerland

R. A. HOUZE JR.

Atmospheric Sciences, University of Washington, Seattle, Washington

H. HUNTRIESER

Atmospheric Science, Swiss Federal Institute of Technology, Zurich, Switzerland

(Manuscript received 29 April 1994, in final form 18 October 1994)

ABSTRACT

The structures of severe mesoscale precipitation systems (MPS) in Switzerland have been classified by analyzing radar images obtained over a 5-yr period. Severe MPSs were defined to be those producing most of the damage on days on which at least 5 (out of 2400) communities reported water and/or at least 20 reported hail damage. Of 94 MPSs selected, 82 had radar reflectivity of 47 dBZ or greater and were referred to as mesoscale convective systems (MCS). The 12 remaining MPSs consisted of less intense, long-lasting, and widespread frontal or orographic rainfall.

Subclasses of MCSs were defined according to their internal arrangements of cell complexes (CC). A CC was defined as an echo contour of 40 dBZ surrounding echo maxima of at least 47 dBZ. Four general categories of organization were found: isolated CC, a group of CCs, and a broken or continuous line of CCs. All categories can be purely convective at the mature stage, or the CCs may be juxtaposed with a stratiform precipitation area, usually behind moving convection. The stratiform region often developed as a decaying convective area. These categories were examined in relation to sounding, surface mesonet, synoptic weather type, and severe weather information.

In 26 cases, the MCS had "leading line–trailing stratiform" structure. These MCSs were graded according to a classification scheme previously used to characterize spring rainstorms in Oklahoma. Only moderately and weakly classifiable storm systems occurred in Switzerland. The mountain barriers apparently interfered with the airflow such that MCSs were prevented from having enough time and space to develop to a higher degree of organization as is possible over the relatively flat terrain of Oklahoma. In addition, the instability and the wind shear in the Swiss storm environment was found to be weaker.

1. Introduction

Heavy rain and hail are important natural hazards in Switzerland. Heavy rain produces floods and landslides, and hail damages property and crops. Research into the nature of the convective storms producing such disasters has been ongoing since weather radars have been available (e.g., Donaldson 1958; Douglas and Hitschfeld 1959). Most of this work has emphasized the individual thunderstorm elements in which the hail and rain are concentrated. In the 1970s and 1980s, hailstorm research in Switzerland was undertaken in the framework of hail suppression experiments (Federer et al. 1986). As part of this work, the relation between radar-derived hail kinetic energy and hailpad measurements (Waldvogel et al. 1978; Waldvogel and Schmid 1982) as well as between radar reflectivity measurements and hail damage (Schiesser 1990) were obtained. More recently, the research has shifted toward the understanding of the basic dynamical processes that govern Swiss storms but still focuses on the behavior of individual hail cells. Schmid et al. (1992) examined the kinetic energy of the hailfalls from individual cells. Houze et al. (1993) presented a storm climatology showing that, in contrast to storms in the United States, 50% of Swiss thunderstorms are left moving; they used case study analysis and numerical modeling to investigate the dynamics of the left and right movement of the storms.

Thunderstorm cloud elements commonly occur as part of organized mesoscale cloud systems (Houze 1993, chapter 9). A preliminary climatological investigation of the mesoscale organization of precipitation systems affecting Switzerland has been presented (Schiesser and Houze 1991), and case studies of meso-

Corresponding author address: Dr. Hans-Heinrich Schiesser, Atmospheric Science, ETH-Hönggerberg, CH-8093 Zurich, Switzerland.

scale precipitation systems in a nearby region (southern Germany, northeast of Switzerland) have been undertaken by Meischner et al. (1991) and Hagen (1992). However, the nature of the mesoscale organization of Swiss storms has not heretofore been extensively explored. In particular, little has been done to document the extent to which the individual hailstorm elements occur in isolation or in organized groups or lines.

If storms producing severe weather in Switzerland are to be better understood, modeled, and predicted, a knowledge base is needed that describes the mesoscale structure and organization of the storms. This background knowledge is also important to estimate the impact of regional climatic changes on the severe storm systems. Therefore, the following analysis is also done in the framework of a recently introduced Swiss National Research Program (NRP31) entitled "Climatic Changes and Natural Disasters."

In the first part of this paper, we document the mesoscale structure of precipitation in Switzerland. We concentrate on the area north of the crest of the Alps, where precipitation coverage is documented by two radars and a network of automatic weather stations operated by the Swiss Meteorological Service (Schweizerische Meteorologische Anstalt, or SMA) and where severe weather is well documented by news media and insurance companies. We construct a 5-yr climatology (1985–89) of the mesoscale organization of the precipitation producing severe hailstorms and excessive rain. This climatology distinguishes five general types of radar structures that occur repeatedly, determines details of the radar echo structures in each of the five categories, and relates these structures to soundings, surface mesonet measurements, synoptic weather type, and severe weather information.

The second part of this study is similar in approach to that of Houze et al. (1990, hereafter HSD), who examined the mesoscale structure of major springtime rainstorms in Oklahoma. By examining radar echo patterns for six consecutive wet seasons, they found the major rain events always to be composed of a combination of convective and stratiform precipitation. In some two-thirds of the cases, the precipitation on radar had a tendency to be in the configuration of a "leading line and trailing stratiform" region. However, the tendency toward this high level of mesoscale organization ranged from rather weak to very strong. In the remaining one-third of cases, the precipitation was in an unclassifiable arrangement of convective cells and stratiform precipitation. The examination of all these radar echo patterns led to a clearer knowledge of the spectrum of storm types that bring heavy rain to Oklahoma. The Swiss storm systems selected for our study are treated in the same manner; that is, they are classified according to the scheme of HSD. This procedure allows us to compare the organization of storms occurring in the mountainous and hilly region of Switzerland with mesoscale convective systems in the generally flat region of Oklahoma.

2. Study area, data, and definitions

a. Area and period of study

Figure 1 shows the location of the *study area.* It is situated within the area covered by two operational weather radars and has a size of about 37 000 km^2, of which 25 000 km^2 lies within Switzerland. The remainder of the region lies within eastern France and southern Germany. The area is restricted to the region north of the alpine ridge since precipitation to the south is blocked from radar surveillance by the high mountains (Joss and Kappenberger 1984). The topography of the region is depicted in Fig. 2.

The present investigation covers the 5-yr period 1985–89. All 12 months of each year are considered, not just the warm season as in the study of HSD. However, the majority of the cases belong to the warm period of the year (May–September).

b. Radar data

Since 1979, the SMA has operated two 5-cm-wavelength weather radars 24 h a day in Switzerland (Joss and Waldvogel 1990). These two radars cover a volume of 558 km × 428 km × 12 km. Figure 1 shows the two radar sites and the combined observational area, which reaches into France in the west, whence large precipitation systems usually move into Switzerland. The radar images are recorded and archived on 16 mm film at 10-min intervals. Each image shows three projections (horizontal map of reflectivity and west–east and north–south vertical cross sections). The pixel size in the horizontal is 2 km × 2 km and the vertical bin size is 1 km. Each pixel contains the maximum radar reflectivity in each vertical column or horizontal strip. For display purposes, the reflectivity is converted to rainfall rate R through the relation $Z = 300R^{1.5}$, where Z is the equivalent radar reflectivity factor (Z is expressed in dBZ, which we will refer to simply as "reflectivity"). The reflectivity values (and corresponding rain rate) are color coded in seven steps with the threshold intensities indicated in Table 1.

Although the radar-observed area in Switzerland is about the same size as that used by HSD (Fig. 1 of HSD), our study area is considerably smaller since it is restricted to the northern part of Switzerland, where damage data are available. The radar data are used to identify and analyze the important mesoscale precipitation systems (MPSs) that affect the study area during periods of significant hailfall and/or flooding (subject to specific criteria to be described).

c. Damage data

We use two sources of damage information to determine the severity of an MPS. 1) Reports of damage

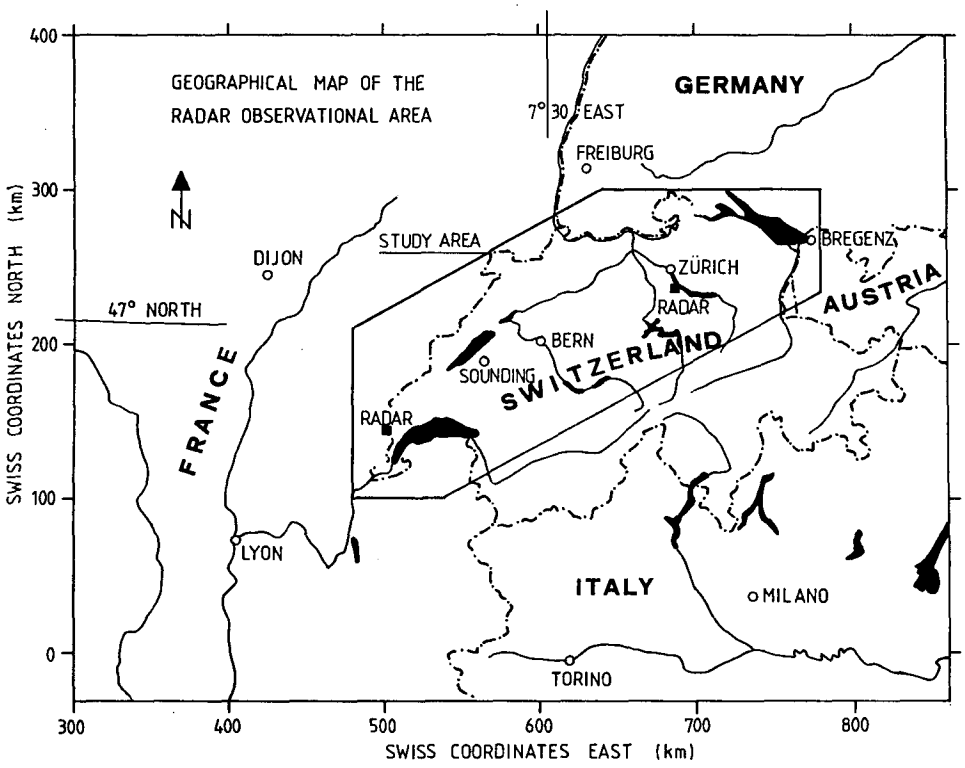

FIG. 1. The combined observational area of two Swiss weather radars. Radar data are recorded for the entire rectangular area. The irregular hexagon is the boundary of the study area. The coordinate system, which is used in Switzerland (capital Bern 600 km, 200 km), indicates the scale.

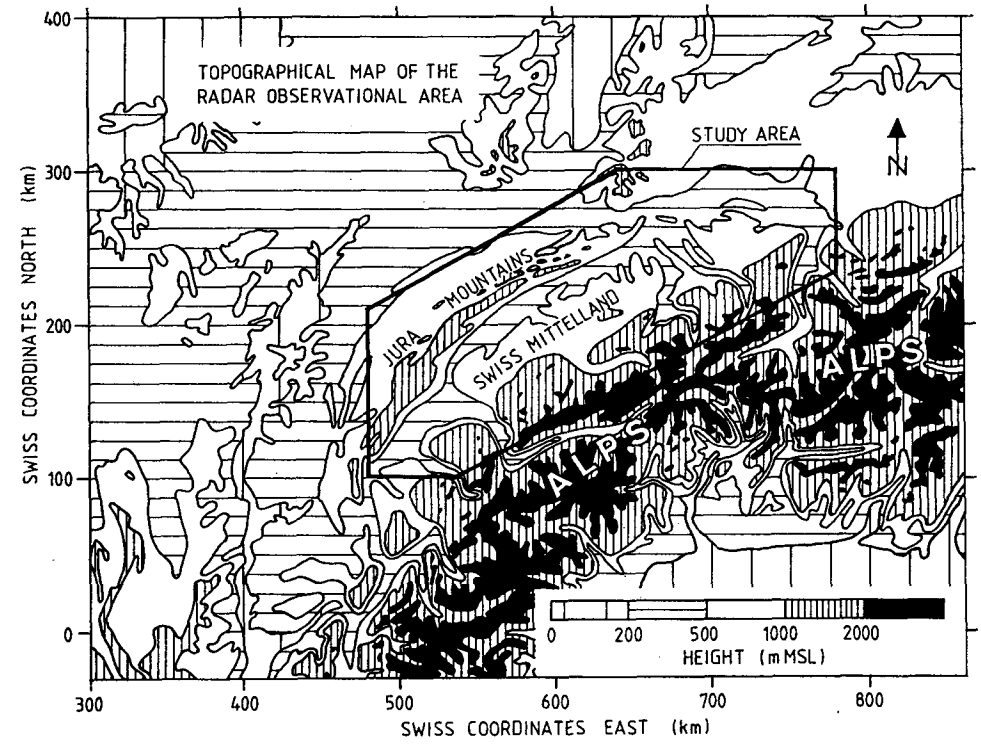

FIG. 2. The topography of the observational area shown in Fig. 1.

TABLE 1. Radar echo intensity levels used in archived data of SMA radars.

Level	Rain rate (mm h^{-1})	Reflectivity (dBZ)	Figure hatching
1	0.0–0.3	<17	not used
2	0.3–0.9	17–24	not used
3	1.0–2.9	25–31	□
4	3.0–9.9	32–39	▨
5	10.0–29.9	40–46	▥
6	30.0–99.9	47–54	□
7	≥100	≥55	■

caused by water, collected routinely since 1972 at the Swiss Federal Institute of Forestry Research from more than 500 newspapers. From the news information, the type of weather (either thunderstorm or intense rain, long-lasting rain, or snowmelt with rain), the type of damage (flooding, landslide, or both), and the severity of damage (small, medium, or heavy) are indicated for every community. Summaries are published yearly (e.g., Zeller and Röthlisberger 1988). 2) Listings of hail days (having hail damage in agriculture) by community, compiled yearly by the Swiss Hail Insurance Company. A hail day means that at least one report of hail damage (to one crop or field) was received by the hail insurance company. No further information is given about the extent of hail damage. For that, one has to investigate the single damage reports (Schiesser 1990).

The portion of the study area within the Swiss border contains over 2400 communities for which damage information is available (Fig. 3a). Figure 3b shows, as an example, the locations of 134 communities that reported hail damage on 1 July 1987. Figure 3c shows the 39 communities that suffered damage caused by water on the same day. Since the number of communities in the study area is large and the average size of a Swiss community is small (about 10 km^2 on average, Schiesser and Willemse 1992), the number of reporting communities is taken as a measure of the severity of a day or an MPS. The larger the number, the more severe the case, independent of the actual size of the reporting communities or the precise percentage of damage to the agriculture. For the 5-yr period and within the area of study, at least one community reported some water damage on 139 days and hail damage on 445 days.

d. Definition and selection of severe mesoscale precipitation systems

To select a meaningful yet manageable sample of days with damage reports, we define a severe precipitation day (SPD) as a day within which at least 5 Swiss communities suffered damage by water and/or at least 20 communities were damaged by hail. One or more MPSs, which developed within or moved into the study area, may have been responsible for the damage during an SPD. The years 1985–89 included 120 SPDs. Of these, 7 had no radar data, and 19 had radar data of insufficient quality for this study (some important images were missing, or only one radar was operating) and are disregarded, leaving 94 SPDs for this study.

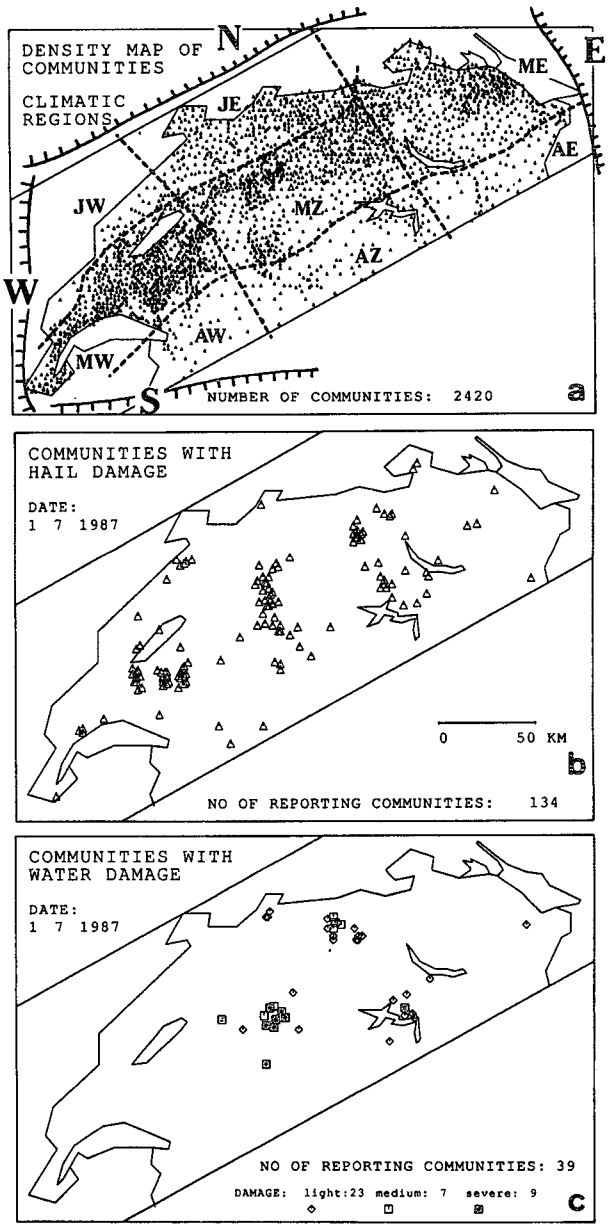

FIG. 3. (a) Density map of the Swiss communities north of the alpine ridge. The symbol represents the center of the community from which hail and water damage information are available. The two-letter abbreviations refer to climatic–topographic regions delineated by dashed lines. The names corresponding to the abbreviations are explained in the appendix. (b) Locations of communities of which at least one policy holder reported hail damage to the hail insurance company on 1 July 1987. (c) The same as (b) but for water damage.

The SPDs are stratified into days with intense or less intense precipitation. To designate a day as *intense,* one radar image during an SPD must contain echo of intensity of at least 47 dBZ ($\sim$30 mm h^{-1}). Otherwise the day is designated as *less intense.* This criterion separated well the intense rain and hail cases from long-lasting widespread stratiform rain cases. Twelve SPDs were less intense, whereas the remaining 82 cases were classified as intense. A particular MPS in which an echo of at least 47 dBZ occurs is referred to as a mesoscale convective system (MCS).

To compare the organization of MPSs in Switzerland with those in Oklahoma, the same MPS definitions used by HSD are adopted here. HSD considered an MPS "to be a distinct group of echoes or contiguous area of radar echo that extended spatially over horizontal distances of approximately 100 km or more at time of maximum extent and exhibited time continuity over several hours." In the following, the area enclosed by the radar contour of 25 dBZ ($\sim$1 mm h^{-1}) is taken to define a unique precipitation system, if it has a distinct separation from any other radar echo area of the same intensity at the same instant. If a system splits, the largest or most severe part is tracked further. In case of a merger, all the merging parts belong to the system that was largest or most severe at the time of the merger.

Since on an SPD day one or several MPSs can exist (the 94 days showed a total of 338 individual MPSs, average 3.8), the number of cases had to be reduced further to obtain a manageable set of systems. Therefore, only the most severe MPS, defined as the one affecting the largest number of the day's reporting communities, was included in the analysis. Hence the number of severe systems examined is equal to the number of SPDs. Of the 94 MPSs analyzed, 9 showed a maximum extent of less than 100 km (ranging from 53 to 92 km) and thus did not strictly satisfy the HSD definition of MPS. However, all 94 systems are included and treated as MPSs in the following analysis. Often, one MPS dominated the damage in a particular SPD. In 32 cases, a single MPS (34%) was responsible for all of the damage during a particular SPD. In another 25 cases (27%), the investigated MPS accounted for at least 75% of the reporting communities, and in the remaining 37 cases (39%) the investigated MPS was responsible on average for 53% of the day's damage.

e. Additional meteorological data

1) SYNOPTIC WEATHER INFORMATION FROM SMA

Daily information about the synoptic weather situation was obtained from the Annales of the SMA (yearly summary of meteorological data). Of relevance for this analysis are 1) occurrence/nonoccurrence of fronts: for example, a day was considered to be cold frontal if a cold front occurred on that day or prefrontal if a cold front passed through the next day—otherwise an "air-mass" day was declared; 2) the time of passage of the front through Switzerland (first or second half of the day); and 3) the type of air mass affecting most of Switzerland at 1200 LST (1100 UTC). These airmass types are classified and recorded by the SMA in the traditional categories; arctic, maritime polar, continental polar, maritime tropical, and continental tropical, which are a qualitative interpretation of the probable origin of the air at the surface (Petterssen 1956b, p. 25).

2) SOUNDING DATA

The routine soundings from Payerne (Fig. 1, only station in Switzerland) were used to characterize the environment of the MPSs north of the Alps. For MCSs, usually the sounding preceding the time of development of the most severe MPS of the day was used (either 0000 or 1200 UTC), except for cases with start time only 1 h before the release time of the sounding (if not contaminated by precipitation). For one intense case, which passed through the study area at midnight (2130–0100 UTC) the 0000 UTC sounding was taken. During 7 SPDs (out of 82), the area in which the most severe MCS developed was evidently altered by the precipitation of an older system. Those seven days were omitted from the comparison of sounding parameters. For the long-lasting less intense cases, the closest sounding to the start time was taken, because of the more stable environmental conditions in such precipitation regimes. On average, the sounding was started at 2 h ($\pm$4.8) before the first echo of 25 dBZ (1 mm h^{-1}) appeared in cases of a less intense MPS and 3.9 h ($\pm$3.6) in cases of an intense system, respectively.

3) MESONET

At 30 automatic stations (with elevations all less than 1500 m MSL), measurements of basic meteorological variables are obtained by the SMA every 10 min within the boundary of the study area, the same frequency as the data from the radars. For each station in and around the damage area affected by the most severe MPS of a day, we have compiled the following mesonet variables: 1) the maximum rain accumulation during 1 h; 2) the maximum 10-min amount of precipitation; 3) the peak wind gust during the lifetime of the MPS; 4) the maximum mean hourly wind speed, and 5) the maximum number of lightning strikes, measured within a radius of 5 km. For this analysis, the value of the station with the maximum of all involved stations is recorded to obtain the most extreme values measured within the MPS by the automatic network.

f. Variables used to describe the mesoscale precipitation systems

On the basis of the synoptic data, soundings, radar data, surface mesonet, and damage reports, several variables have been defined and their values recorded

for each of the 94 MPSs. A complete listing of the variables and their definitions is given in the appendix. All time information is given in UTC (local time is UTC +2 h during April–September +1 h otherwise).

3. Mesoscale organization

a. *Definitions*

The radar structures of the 12 less intense cases (defined in section 2d) are not subdivided into more detailed categories since most of them consisted of long-lasting widespread stratiform rainfall with relatively low intensity, which did not clearly show features like rainbands (Houze and Hobbs 1982; Browning 1990; Houze 1993, chapter 11) with the available radar intensity intervals at 7–8-dBZ intervals (Table 1). For the 82 intense MCSs, different radar structures are well indicated by the five highest intensity levels, and the organization of an individual MCS is categorized according to its internal structure as shown by these levels (Fig. 4).

The damage producing entity in an MCS is the *cell* of hail or intense rain. A cell is defined as a region enclosed by a 47-dBZ (30 mm h^{-1}) radar echo contour. The 47-dBZ intensity contour corresponds closely to the reflectivity level (45 dBZ) used operationally to define a cell in the Swiss hail suppression experiment Grossversuch IV (Federer et al. 1986).

We call the region of echo bounded by the 40-dBZ radar reflectivity contour and containing one or more cells during the mature phase of storm development (peak echoes of at least 47 dBZ) a *cell complex* (CC). As indicated in Fig. 4, a CC sometimes (but not always) consists of cells arranged or oriented in a line.

We consider the outer boundary of an MCS to be a closed contour of 25 dBZ within which are found one or more CCs. MCSs, so delineated, are then classified into four categories of CC organization:

The first category of MCS contains an *isolated* CC.

The second category of MCSs contains a *group* of CCs, in which multiple closed contours of 40 dBZ are separated from each other and arranged with no apparent organization within the area of greater than or equal to 25-dBZ echo intensity. No line structure is evident during the mature phase of its lifetime, and the size of an individual CC is similar to that of an isolated CC.

The third category is a *broken line* of CCs. Two or more CCs are arranged in a line more or less perpendicular to the apparent direction of movement of the whole line. The 40-dBZ radar echo contours of the individual CCs are separated, and the size of an individual CC is similar to that of an isolated CC.

The fourth category is a *continuous line* of CCs. The area of precipitation with radar reflectivity of at least 40 dBZ is elongated in one direction, usually two or more cells appear within it, and the length-to-width ratio of the elongation is more than about 3:1.

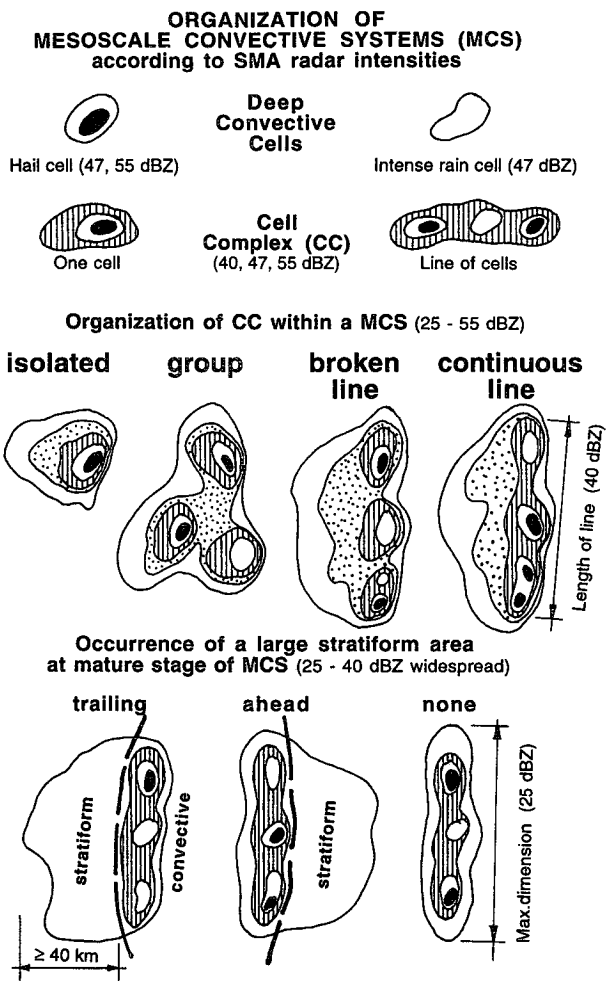

FIG. 4. Schematic drawings of the organization of the mesoscale convective systems (MCS). The radar intensities are given in dBZ. The movement of storm systems is from left to right.

More often than not, one of the cells in a CC exhibits a radar reflectivity value of more than 55 dBZ (100 mm h^{-1}) and, as such, is expected to produce severe weather in a system. Waldvogel et al. (1978) showed that for Swiss storms a threshold of 55-dBZ radar reflectivity is associated with hail on the ground. The location of highest radar echo intensity is also in good agreement with the corresponding damage information, especially hail damage on the surface (Schiesser and Willemse 1992). The time and location of the peak echo within a CC usually coincide with the occurrence of damaging hail or intense rainfall.

Another element of organization is whether or not a sizable *stratiform* precipitation area is present in a mature MCS. HSD found that all the major rain events in their Oklahoma study exhibited stratiform precipitation areas, and the spatial arrangement of convective and stratiform regions was a useful indicator of MCS organization. In this study, a stratiform region is identi-

fied in one of three possible situations. It is a nonconvective echo about 40 km in dimension and is located on either the leading or trailing side of a region of active convective precipitation, or it appears as part of the dying phase of the convective life cycle. This latter type of stratiform echo formation—from weakening convection—is described by Houze (1981) and Houze (1993, chapter 6). If the convective organization is a broken or a continuous line and a trailing stratiform area is observed, then such a system is called "leading line/trailing stratiform" and corresponds to the "classifiable" type of MPS structure analyzed by HSD. All other types are assumed to belong to the "unclassifiable" category according to the same authors.

The types of radar echo organization just described and illustrated in Fig. 4 are often not evident during the entire lifetime of an MPS. The structure of a given MPS is based on its echo pattern at or around the most intense phase (mature stage) of the system and must be clearly visible for about half an hour (three successive radar images). Other types of echo patterns are often seen in the growing phase of a system, before the system has become organized, which is often after mergers of various systems.

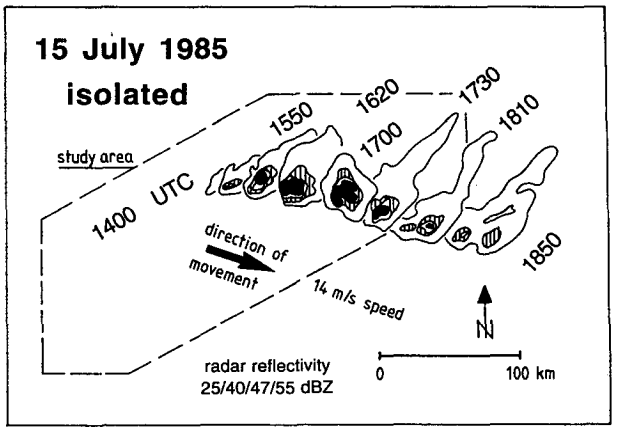

FIG. 5. Example of a mesoscale convective system of the "isolated" type of organization on 15 July 1985. The contours are given in time steps of about half an hour. The direction and speed of movement of the system is indicated. Radar echo intensity levels are those described in Table 1.

b. *Examples*

Figures 5–8 show examples from the 1985–89 dataset of mesoscale organization for each of the four MCS categories. The figures illustrate the most severe hail event in each category—that is, the case with the largest number of hail damage reporting communities.

Figure 5 illustrates the isolated type of MCS organization, which consists in this case of only one large hail cell. The cell developed in situ at 1400 UTC 15 July 1985, reached its maximum intensity (>55 dBZ) around 1700 UTC, and left the study area at 1810 UTC. This hail cell caused damage in 88 communities along its path. It was a precipitation system that just met the requirement for an MPS—that is, maximum extent of the 25-dBZ echo area exceeded 100 km. The maximum dimension, measured at 1730 UTC, included the small elongated area of the anvil. The MCS was the second system (out of four) on that particular day.

Figure 6 shows a more complex MCS structure. It illustrates the group organization of CCs. Six stages in its development are shown. The dashed boundary line encloses the study area, while the circle, having a radius of 200 km, indicates the size of the Oklahoma study area of HSD. At 2030 UTC (Fig. 6a), two broken-line structures were visible in the west and to the north of the study area within the closed boundary of the 25-dBZ radar contour. By 2130 UTC (Fig. 6b), the northern line had rearranged itself into a group organization, and a hail cell had developed (highest intensity level) within CC A. At the same time, CC B was growing. Around 2220 UTC, CC B also contained hail cells and was moving in an eastward direction at a relatively high speed of 19 m s^{-1} (Fig. 6c). The group character of the MCS was best seen around 2320 UTC, when B, the largest CC, reached its maximum size, and CC A was already in its decaying phase (Fig. 6e). The CCs A and B were jointly responsible for hail damage in 98 communities. In the decaying stage of the MCS (Fig. 6f), the CC organization showed a more continuous-line feature. The maximum dimension of the overall contiguous radar echo seen in Fig. 6b was almost 400 km. This MPS was the second of three on this day.

An example of an MCS with the broken-line type of organization passed through Switzerland on 23 July 1986 (Fig. 7). It was the most severe MCS of the investigated period (1985–89) in terms of hail damage. The whole complex, with several hail cells, was responsible for damage in 248 communities, or about 10% of all the communities within the study area. Broken-line B moved in from the west around 1450 UTC (Fig. 7a). Ahead of B was a large stratiform area with embedded areas of higher reflectivity, which were not sufficiently intense to be called CCs. An isolated CC, labeled A, was in an early phase of development in situ. The system moved with a speed of 19 m s^{-1} toward the northeast, parallel to the alpine ridge (Fig. 2). New squall lines (C, D, and E) moved into the study area from the west and were all present at 1720 UTC (Fig. 7f). The most active stage of development was reached at 1630 UTC (Fig. 7d).

The continuous-line type of organization is illustrated in Fig. 8. On the southern end of this huge MCS was a large CC with multiple convective cells. During the night of 1/2 August 1988, it passed

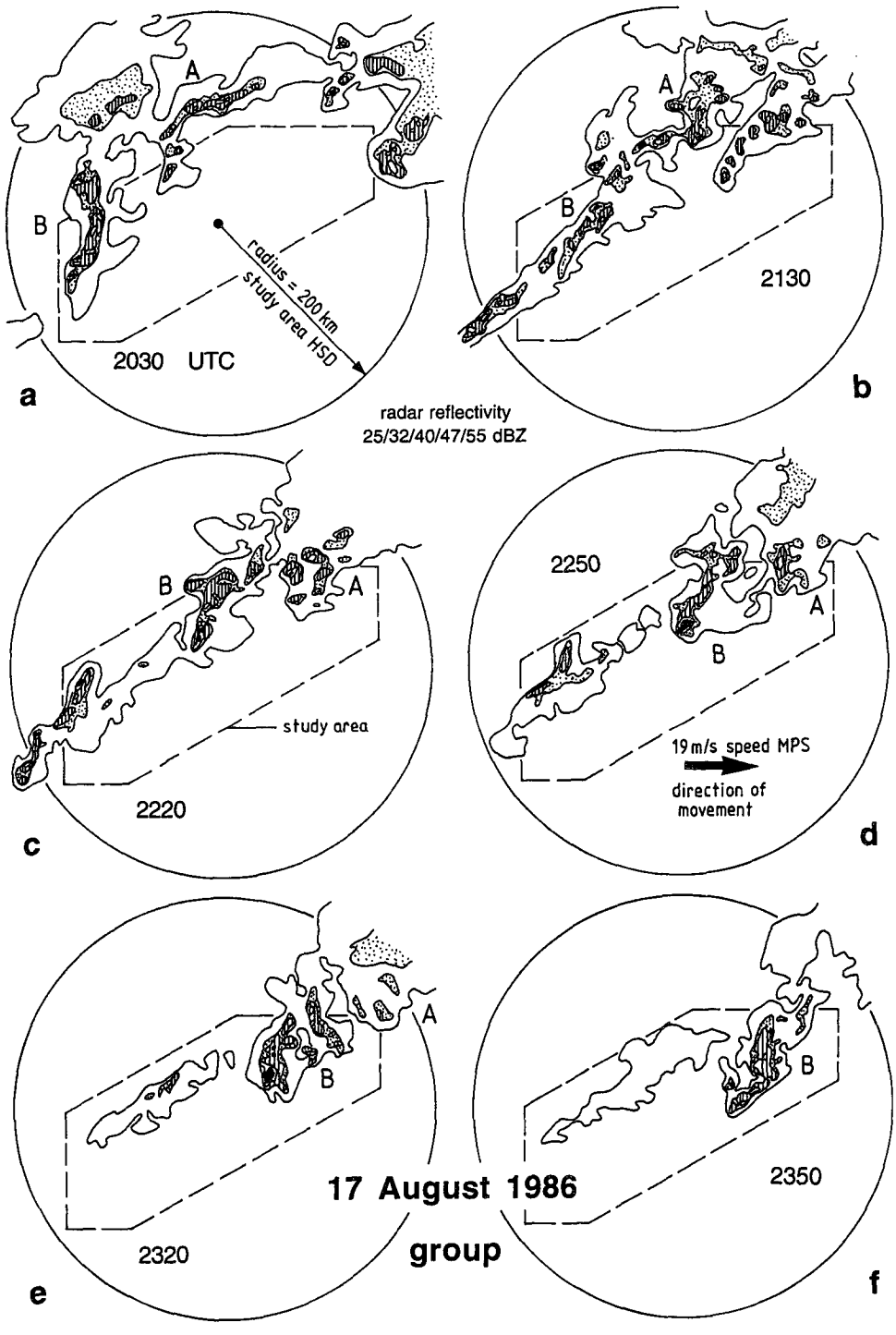

FIG. 6. Example of a mesoscale convective system of the "group" type of organization on 17 August 1986. Six stages of development are shown. The dashed hexagon encloses the study area. The circle of radius 200 km indicates the size of the study area used by HSD in their study of Oklahoma storms. The direction and speed of movement of the system is indicated. Radar echo intensity levels are as described in Table 1.

through the northern part of the study area, where it was responsible for hail damage in 150 communities. A stratiform region stretched to the north and ahead (east) of the convective activity. The full area of echo of at least 25 dBZ is shown only at 0030 UTC. At the other times only the continuous-line complex

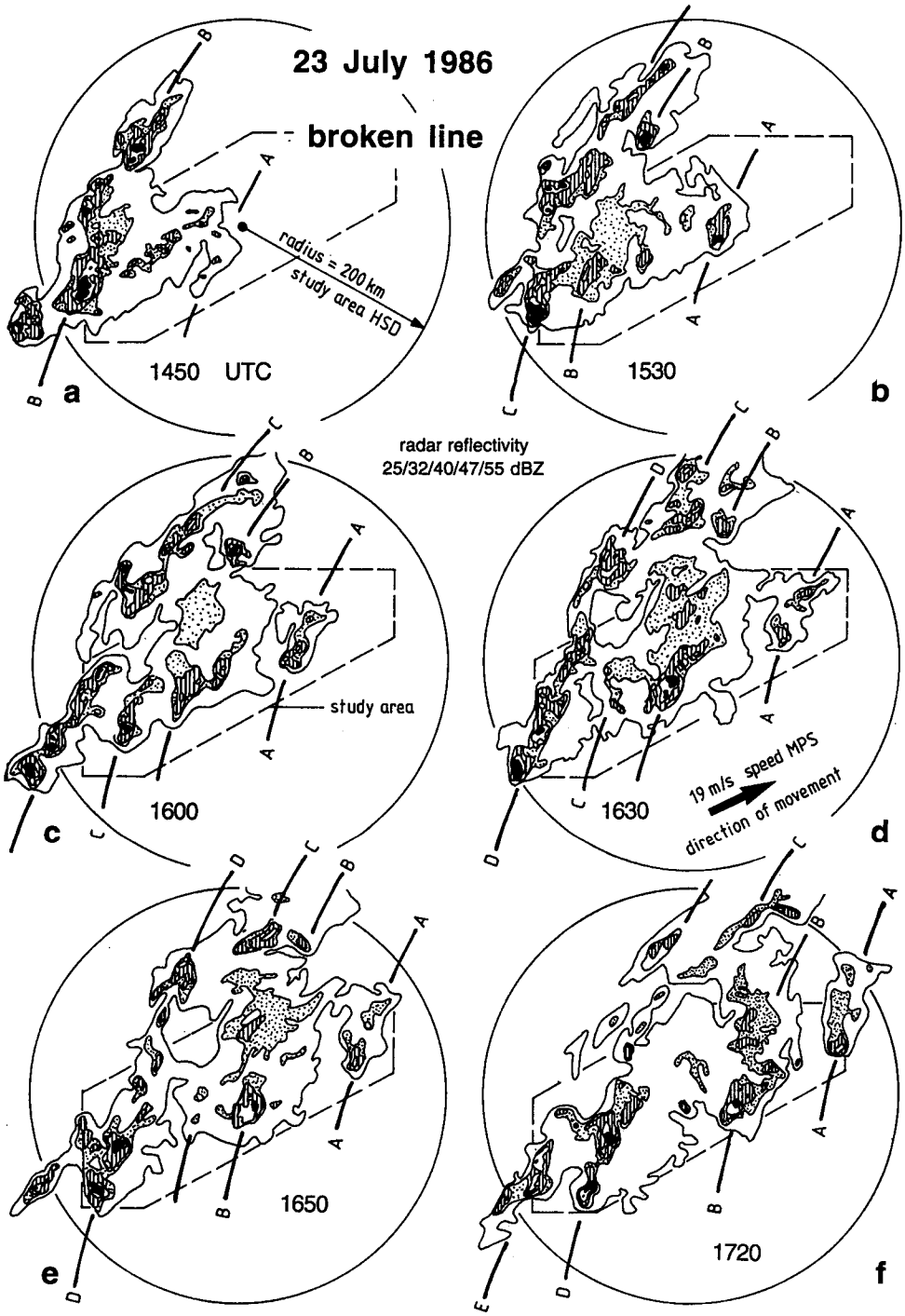

FIG. 7. As in Fig. 6 except for an example of a mesoscale convective system of the "broken line" type of organization on 23 July 1986. Several successive lines are marked with the letters A to E.

is drawn in full, and the stratiform parts overlap. The maximum extent of the MPS toward the north is not determinable because of the lack of radar information beyond the edge of the image. The storm entered the study area around 2200 UTC from the west (on 1 August 1988), already as a huge mature system. The hail-producing complex reached its maximum size around 2330 UTC and left the area in the beginning

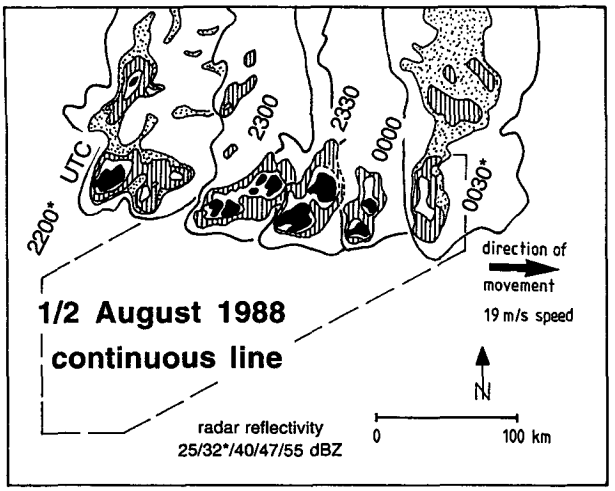

FIG. 8. As in Fig. 5 except for an example of a mesoscale convective system of the "continuous line" type of organization on 1/2 August 1988. Where the images overlap, the latest image is placed on top of the older ones. The radar echoes are cut off in the north by the edge of the region of archived images.

of the decaying phase at about 0100 UTC 2 August 1988.[1]

4. Comparison of the five categories of radar structures

a. Radar variables

Table 2 lists mean values of all the radar-derived variables. Values are given for all MCS cases in column 1 and for the four MCS categories (isolated, group, broken line, and continuous line) in columns 2–5. Columns 6 and 7 are subcategories of the broken- and continuous-line cases, which will be discussed in section 5. Column 8 lists the values for the less intense category. Some of the categories are intercompared by statistically testing whether the mean value of a variable for a given category is significantly different at the 5% level from the mean value of the same variable in another category. The nonparametric Mann–Whitney U-test (Feldman et al. 1987) is used for the testing. Significant differences identified by this test are indicated by footnotes in Table 2. The same method is used in Tables 3 and 4.

1) INTENSE CATEGORIES

Among the 82 MCS cases, the broken-line type of organization was the most frequent and contained on average 3 CCs within the study area. The occurrence of the MCSs in general (all cases, column 1 of Table 2) was evenly distributed over the months of May to August.

Of all cases, 60% developed in the study area (in situ), while the rest moved into the area, mostly from the west-southwest. Figure 9 shows the percentage of events (upper entries in the two-row boxes) that originated or moved into particular climatic regions. The climatic regions are identified in Fig. 3a and associated with the main topographic features indicated in Fig. 2. The cases that moved into the study area as part of a large frontal system can be seen from the one-row boxes (labeled N, W, or S). The second row of the boxes (lower entries) reveals the percentage of cases that exhibited their mature stage (i.e., the instant when the main CC responsible for damage appeared to have the largest extent of high radar reflectivity) in a particular climatic region.

Figure 9 shows that the majority of the MCSs developed in the western part of the study area. The isolated MCSs showed a strong preference for development in the eastern Jura Mountains (JE), while the group MCSs tended to form in the western Jura (JW). A large fraction of the MCSs with line organization moved in from the west–southwest. The mature stage (lower entries in the boxes of Fig. 9) was reached for a high percentage of cases in the central Mittelland (MZ), where the broad countryside of low rolling hills allowed for relatively undisturbed development of the CCs. Only the mature continuous-line structure occurred equally in the entire Mittelland. In addition, the most important relationships (at least 5% of all events) between climatic-topographic regions—that is, the path from the region of origin to the region of mature stage—is depicted in Fig. 9 by arrows, which point mainly toward the central Mittelland.

On average the start time of an MCS was around 1300 UTC. It took about 3 h on average for a system to reach the maximum stage of development (time CC). A scatterplot of the relationship between start time and time CC (Fig. 10) stratifies the 49 in situ cases into the 4 types of MCS organization. Only the in situ cases are considered since they are the only cases for which the actual start time can be obtained, in contrast to the systems which moved in. A second-order regression line is drawn in Fig. 10 and shows that the later the start time, the quicker the development of the system to maturity.

The average lifetime of an MCS within the study area was nearly 8 h, about 1.3 h shorter in the case of an MCS with an isolated CC. The lifetime can vary considerably (Fig. 11a in situ cases, Fig. 11b all cases). Only 5 in situ cases and 11 cases altogether exceeded a lifetime of 10 h. Those cases had a rather long decaying phase of stratiform precipitation. In Fig. 11, the lifetime is plotted versus the maximum dimension of the area of radar echo of at least 25

[1] The second author, in a state of jet lag, was awakened at about midnight by the thunder from this storm after having arrived in Zürich on 1 August 1988 to spend a year at ETH.

TABLE 2. Mesoscale precipitation system (MPS) characteristics derived from radar data (number, percentages, and mean values). Columns 1–7 refer to the intense category of MPSs, referred to in the text as mesoscale convective systems (MCSs). Columns 6 and 7 refer to the subcategories of line structure referred to in the text as "leading line–trailing stratiform" (ll–ts) and "no trailing stratiform" (nts). Column 8 contains information on the less intense category of MPSs.

Column	1	2	3	4	5	6	7	8
				Intense				Less intense
Variables	All	Isolated	Group	Broken line	Cont. line	ll–ts	nts	All
Number/% of cases	82/100%	22/27%	17/21%	29/35%	14/17%	26	17	12
Month (%)								
May	25.6	27.3	17.6	34.5	14.3	19.2	41.2	Jan (1), Feb (1)
June	22	36.4	17.6	10.3	28.6	23.1	5.9	Mar (1), Apr (2)
July	25.6	22.7	47.1	24.1	7.8	23.1	11.8	May (1), Jun (2)
August	22	9.1	11.8	31	35.7	26.9	41.2	Jul (2), Sep (1)
September	3.7		5.9		14.3	7.7		Oct (1)
Origin (number/%)								
In situ	49/60%	18/82%	11/65%	13/45%	7/50%	9/35%	11/65%	1/8%
Moves in	33/40%	4/18%	6/35%	16/55%	7/50%	17/65%	6/35%	11/92%
Start time (UTC)	12.9	12	14.1	13.1	12.2	12.7	13.4	12.3
Lifetime (h)	7.7	6.7	8.2	8	7.9	8.1	7.6	18.9
Speed ($m\ s^{-1}$)	9.3	8.8	8.8	9	11.3	10.7	8.1	6.8
Stationary (number)	8	2	0	5	1	2	4	3
Max. dimension (km)								
All cases	186	137[a]	207	212	182	210	191	345
Only study area	141	113[a]	144	169	144	175	143	
Merger (number/%)								
Yes	45/55%	8/36%	13/77%	18/62%	6/43%	15/58%	9/53%	2/17%
Length of line (km)				135[b]	90	120	124	
No. CC	2.1	1	2.7	3	1.4	2.3	2.6	
Time CC (UTC)	16.1	15	16.6	16.6	16.9	16.5	17	
Dimension CC (km)	52	35	46	55	79[c]	69	54	
Organization CC (number/%)								
Isolated cell	45/55%	19/86%	11/65%	13/45%	2/14%	6/23%	9/53%	
Line of cells	37/45%	3/14%	6/35%	16/55%	12/86%	20/77%	8/47%	

[a] sign. smaller than other intense categories
[b] sign. larger than cont. line
[c] sign. larger than other intense caretories

dBZ, which is significantly smaller for the isolated type of organization for all cases ($p \leq 0.009$) as well as for in situ cases ($p \leq 0.024$) compared with the other categories. A good relation between the two variables was found for the isolated cases (regression line in Fig. 11a). This result is useful since most of the isolated cases developed in situ (82%), and it is physically reasonable since the isolated cases merged less frequently with other precipitation areas (see "merger" in Table 2) than in the case of the other three categories. The outlier, with a dimension of 360 km, was physically distinct from the other cases. In its decaying stage, it was a long rainband along the Alps, which had developed from one severe cell. That cell was responsible for flooding, but produced no hail damage.

Figure 11b shows that nine analyzed intense cases did not actually reach the arbitrary minimum size of 100 km to be called an MCS. Most of these cases (seven) are from the isolated category (50–83 km); the other two were from the group (92 km) and broken-line (83 km) categories.

The variation in speed and direction of movement for the single categories is depicted in Fig. 12. The bulk of the systems (79%) moved through the study area from the west-southwest. A total of eight MPSs (10%) were approximately stationary, and only nine traveled from other directions. The continuous-line formation was almost significantly faster than the isolated type of organization ($p = 0.057$).

Table 2 shows that the broken lines were significantly longer than the continuous lines ($p = 0.01$). At mature stage of the MCS, the average dimension of the most severe CC was found to range from 35 km for the isolated, to 79 km of the continuous-line structure that was significantly larger than all other categories ($p \leq 0.01$). The organization of the most severe CC within a system varied from case to case. In 55% of all

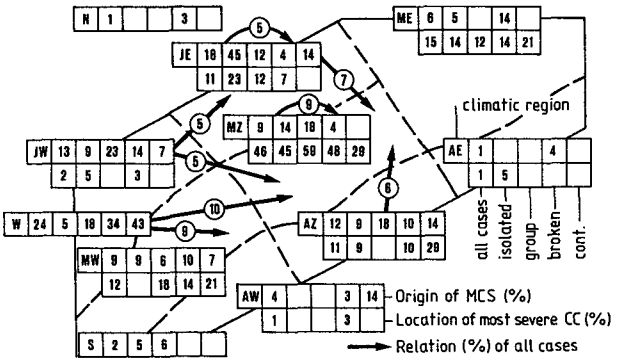

FIG. 9. Origin of the mesoscale convective systems (MCS) and the location of the apparently most severe cell complex (CC). The numbers are given as a percentage of cases and for the four categories of radar structures (isolated, group, broken line, and continuous line). The most important relationships between region of origin and mature stage (location of CC) are indicated by arrows, and the percentage of all cases is given within the circle. Only those relations are indicated that show at least 5% of all cases (four events). The hexagonal region in the background is the study area (Fig. 1). The dashed two-letter abbreviations of the names of the climatic regions are the same as in Fig. 3a and are explained in the appendix.

cases, the CC contained only a single cell at the mature stage.

2) LESS INTENSE CATEGORY

The 12 severe events with long-lasting less intense precipitation that were responsible for flooding (no hail) occurred any month of the year and any time of the day (column 8, Table 2). They usually moved into the study area from the west or northwest. They moved relatively slowly (7 m s^{-1}) through the study area or were blocked by the higher mountains of the Alps. They precipitated for an average time of 19 h (minimum 7 h, maximum 28 h), compared to about 8 h for an intense system. They decayed in situ (seven cases) or left the study area in the east (five cases). For 3 cases, no speed could be attributed to the MPSs because of the lack of distinct radar features to be followed;

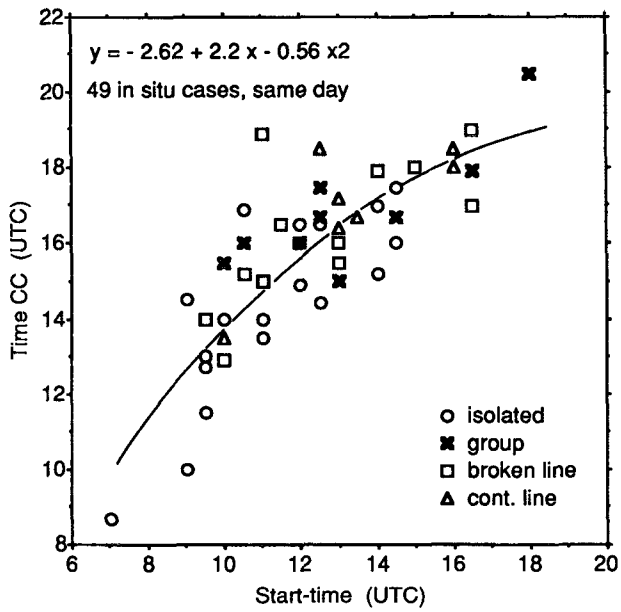

FIG. 10. Scatterplot of start time of an MCS vs time of strongest cell complex (time CC) in its mature phase, stratified according to the four categories isolated, group, broken, and continuous line. Only in situ cases with the whole life cycle during the same day are shown.

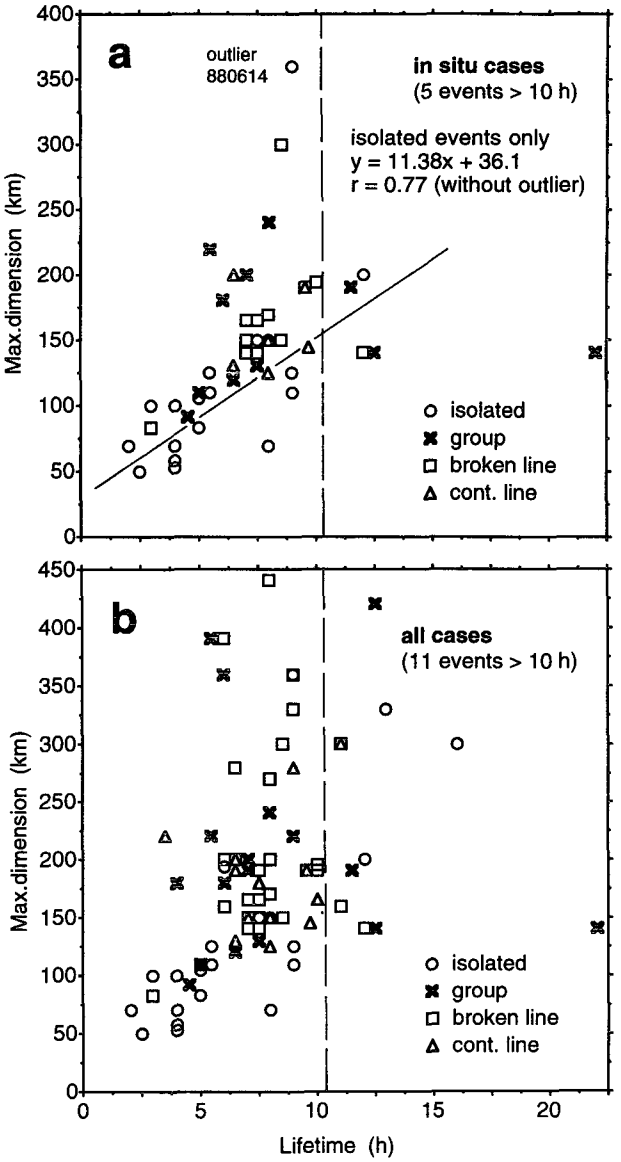

FIG. 11. Scatterplot of lifetime of mesoscale convective system vs maximum dimension of radar echo of 25 dBZ for in situ cases (a) and for all cases (b). Each category of radar echo structure is shown with its own symbol. One outlier (isolated case) is marked and is not used for the regression line of the isolated cases shown in (a).

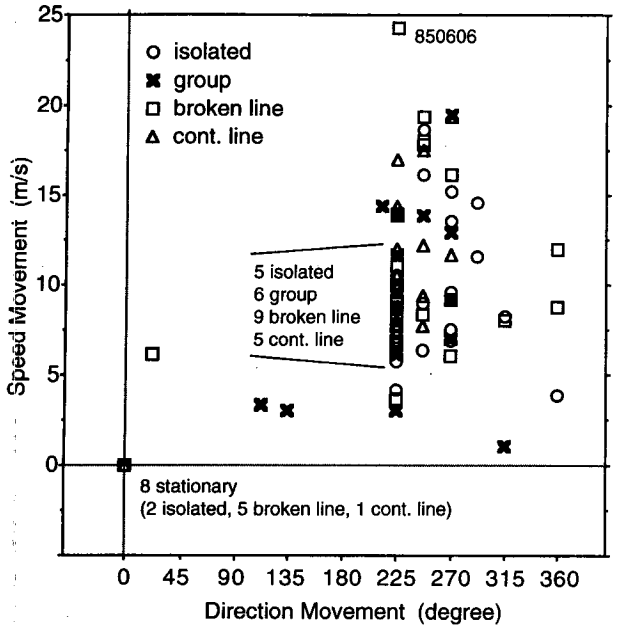

FIG. 12. Scatterplot of direction of movement vs speed of the MCS, stratified according to the four categories of radar echo structure.

therefore, they were labeled stationary. The maximum dimension of such a system was 345 km on average (minimum 125 km, maximum 470 km)—much larger than the convective systems.

b. Weather and sounding variables

1) INTENSE CATEGORIES

Table 3 lists all the synoptic weather and sounding variables in a format similar to Table 2. SPDs occurred most often on cold-frontal days. The remainder occurred in airmass situations, where the local thermal conditions favored deep convection. In 80% of the cold-frontal days, the front passed during the second half of the day. Most of the severe events occurred when a maritime-tropical air mass was over Switzerland. Severe storms are favored when a maritime-tropical air mass lies over Switzerland, and a cold front approaches or passes through the country from west to east (Huntrieser et al. 1994). This situation occurred in about half of all cases.

The sounding variables in Table 3 do not show large differences among the types of organization. However, two aspects of the isolated events are that the mean wind speed between the 3- and 10-km heights was significantly larger than in the group and broken-line categories ($p \leq 0.05$), and the vertical shear in speed between 2.5- and 6-km altitude that was significantly larger than in the continuous-line organization ($p = 0.05$).

Figure 13 contains a scatterplot of the wind speed at 500 hPa versus the shear in speed (ground level to 6 km), stratified into the four MCS categories. The regression line is drawn, and the correlation between the two variables is excellent, which is understandable since the wind speed at ground level was consistently rather low (about 2–3 m s^{-1}, not indicated in Table 3). Therefore, the speed at 500-hPa level might be used as an indicator of the wind shear—at least for the wind environment of Switzerland.

The mean hodographs of the intense categories are shown in Figs. 14a and 14b. The winds on isolated and continuous-line days turned generally clockwise with speed increasing with increasing height. This wind shear environment favored the development of supercells (Weisman and Klemp 1984). The isolated and continuous-line cases had a layer at 4–6 km in altitude where the curvature reversed. This feature made the hodographs similar to the ones that favored left-moving storm development in Switzerland (see Figs. 3b, 5b, and 5c of Houze et al. 1993). The group and broken-line categories showed weaker winds, no turning in their hodographs, and more or less the same speed at higher altitudes. This environment favored ordinary cell development. All of the four hodographs for intense SPDs showed winds of a generally southwesterly direction, in contrast to the less intense days (Fig. 14c), which had a westerly component at low levels and veering winds to northwest at higher levels with increasing speed. This hodograph is consistent with the characterization of the less intense cases as ones of widespread frontal precipitation.

The thermodynamic stratification in the environments of the four MCS categories can be compared by reference to Table 3. The isolated MCSs had significantly lower mean values of the convective temperature ($p \leq 0.001$), height of the 0°C level ($p \leq 0.001$), and the cloud condensation level ($p \leq 0.021$). In addition, the equilibrium level ($p \leq 0.025$) and the convective available potential energy (CAPE, Weisman and Klemp 1982) were significantly lower, whereas the Showalter index (Showalter 1953; modified, see the appendix) was significantly higher for the isolated category ($p \leq 0.023$) in comparison to the line organizations. These quantities all indicate that the isolated cases tended to occur on average in less unstable environments than did the other three types of MCS organization.

2) LESS INTENSE CATEGORY

Half of the less intense events were associated with a passing cold front (Table 3), while one-fourth occurred during airmass situations. Most events developed with maritime-polar air at low levels. Compared with the mean sounding variables of all intense cases, most of the variables differ significantly (Table 3). In particular, the wind speeds and the vertical wind shear

TABLE 3. Same as Table 2 except for mesoscale precipitation system (MPS) characteristics derived from synoptic and sounding data.

Column	1	2	3	4	5	6	7	8
				Intense				Less intense
Variables	All	Isolated	Group	Broken line	Cont. line	ll–ts	nts	All
Synoptic weather								
Number of cases	82	22	17	29	14	26	17	12
Cold-front day (number/%)	45/55%	12/55%	8/47%	17/59%	8/57%	17/65%	8/47%	6/50%
Second (%)	80%	67%	50%	100%	88%	94%	100%	50%
Prefront day (number/%)	10/12%	2/9%	5/29%	2/7%	1/7%	3/12%	—	2/17%
Airmass day (number/%)	27/33%	8/36%	4/24%	10/34%	5/36%	6/23%	9/53%	3/25%
Type of air mass (all days)								
Arctic (%)	—	—	—	—	—	—	—	8
Maritime polar (%)	13	33	12.5	—	12.5	4	—	75
Maritime tropical (%)	67	42	75	82	62.5	73	76	8
Continental polar (%)	4	8	—	6	—	4	—	8
Continental tropical (%)	16	17	12.5	12	25	19	24	—
Cold/Prefront (number/%)								
Maritime tropical	39/48%	7/32%	10/59%	16/55%	6/43%	14/54%		
Sounding								
Number of cases	75	19	14	28	14	26	16	12
Speed 850 hPa (m s^{-1})	6	6.4	5.9	5	7.4	5.8	5.8	8.2
Speed 700 hPa (m s^{-1})	9	10.1	7.9	8.7	9.7	8.7	9.1	14.4[a]
Speed 500 hPa (m s^{-1})	11.3	13.8	10.1	10.5	10.7	10.7	10.5	20.3[a]
Mean speed 3–10 km (m s^{-1})	11.4	14.4[b]	9.1	10.3	11.8	10.5	10.7	20.2[a]
Vertical shear 2.5–6 km (m s^{-1})	5.7	7.4[c]	5.1	5.4	4.9	5.4	5.6	10.7[a]
Vertical shear 0–6 km (m s^{-1})	10.6	12.7	9.4	10.3	9.6	10	10.4	19.8[a]
Convective temperature (°C)	25.2	20.8[d]	27	25.9	28.1	26.9	26.3	17.3[a]
Freezing level (km)	3.4	2.9[d]	3.7	3.5	3.6	3.6	3.5	2.5[a]
CCL (km)	2.3	1.9[d]	2.5	2.3	2.6	2.4	2.5	2
Equilibrium level (km)	9	7.7[e]	9.2	9.3	10.2	9.5	9.3	3.2[a]
CAPE (J kg^{-1})	656	416[e]	625	730	938	841	687	34[a]
Showalter index	−2.2	−1.2[e]	−2.1	−2.6	−2.9	−2.9	−2.8	3[a]

[a] sign. different to all intense cases (column 1)
[b] sign. different to group + broken line
[c] sign. different to cont. line
[d] sign. different to other intense categories
[e] sign. different to broken line and cont. line

(speed) were much higher than on intense SPDs (evident in the mean hodograph in Fig. 14c).

c. *Severe weather and mesonet variables*

1) INTENSE CATEGORIES

Table 4 lists average values of the number of water and hail damage reporting communities per MPS and of five meteorological parameters representing rain, wind, and lightning strikes, as measured by the mesonet. If all MCSs were considered, an average number of 7 water- and 47 hail-damaged communities were counted. The numbers increased, respectively, to 16, if only the MPSs, which fulfilled the water-damage criterion of at least 5 reporting communities, were considered and 61, if only the MCSs, which fulfilled the hail-damage criterion of at least 20 communities, were taken. No significant differences existed among the four categories of radar structures in producing water damage. However, isolated events produced significantly fewer hail damage reports than broken-line events.

The variability of damage is stratified three ways in Fig. 15, which is a scatterplot of the number of communities reporting hail damage versus the number of communities reporting water damage. Figure 15a stratifies the damage according to the four types of MCS structure. For most of the isolated cases, the damage was either caused by intense rain or by hail but seldom both. The group organization tended to produce only hail damage, and the broken-line structure exhibited a lot of mixed cases. The line organizations were responsible for the major episodes of hail damage (more than 100 communities), whereas all categories were able to produce large damage by intense rainfall.

Figure 15b stratifies the variability of damage into cases that developed in situ or moved into the study area. The MCSs with many hail damage reports (more than 100 reports) were all of the type that moved into

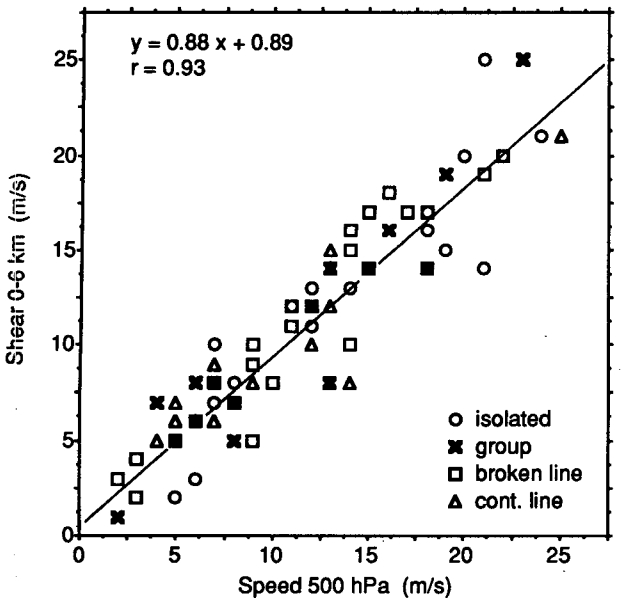

FIG. 13. Scatterplot of wind speed at 500 hPa against vertical shear of wind speed between 0 and 6 km, stratified according to the four categories of radar echo structure.

the country. The two MPSs with the most severe water-damage reports developed in situ. Figure 15c stratifies the variability of damage according to the three indicated categories of synoptic weather situation. The large MCSs with hail (more than 100 communities), which all moved into the study area (Fig. 15b), occurred on frontal days.

Table 4 shows that isolated cases had, on average, significantly smaller maximum number of lightning strikes per hour than all other categories ($p \leq 0.033$); lower maximum hourly rain amount than both line organizations ($p \leq 0.042$); smaller maximum wind gusts ($p = 0.002$) and maximum hourly wind speed ($p = 0.025$) than broken-line cases. The group category lay between isolated and line structure in extreme values. Overall, on average, the line formations were the most violent form of MCS. To illustrate this fact further, the variability of rain rate within the observed MCS population is plotted in Fig. 16. Four MCSs with line organization were responsible for the most extreme amounts of precipitation. Similarly, line organizations exhibited the most extreme wind speeds (Fig. 17).

2) LESS INTENSE CATEGORY

The less intense MPSs showed relatively small values of maximum hourly or 10-min rain amount. However, the duration of precipitation was much greater (about 19 h, Table 2), and the water damage occurred primarily as a result of the cumulative effect of the long-lasting rainfall. Table 4 shows that the 12 MPSs averaged about 18 communities with water damage (compared to 7 for the intense cases). None were associated with hail damage. However, lightning was also registered. This observation indicates, especially for the summer events, that weaker convection may have been involved but was not resolved in the radar images and was not strong enough to be cellular (as defined in this study). The maximum wind gusts can be rather high, on average the same as for isolated MCSs; however, the mean surface wind speed in the mesonet is low (~ 1 m s^{-1}).

5. The "leading line–trailing stratiform" type of organization

a. Trailing stratiform versus no trailing stratiform organization

Since the line-structured MCSs were on average more severe than the isolated or group MCSs (in terms of the number of water or hail damage reporting communities, the extreme values of precipitation amount, wind speeds, gusts, and lightning strikes; Table 4, section 4c.1), we analyzed the two categories of line structure (broken and continuous line) in more detail.

The 43 cases of line structure have been divided into two main categories, labeled as ll/ts and nts in Tables 2–4. These categories are the following:

"Leading line–trailing stratiform" organization (ll–ts), similar to that found by HSD to characterize the mesoscale structure of about two-thirds of the major springtime rain events in Oklahoma. Of the 43 Swiss line-structure MCSs, 26 are found to have ll–ts structure.

Line with "no-trailing-stratiform" structure (nts), which includes 12 cases with no significant stratiform precipitation either ahead or behind the line (the cases indicated as "none" in Fig. 4) and 5 cases in which a stratiform region occurred ahead of the line, possibly as a blowoff feature (the cases indicated as "ahead" in Fig. 4).

Table 2 indicates that only 35% of the ll–ts cases developed in situ, compared to 65% of the nts cases. The ll–ts storm systems moved somewhat faster than the nts storms, and the maximum dimensions were somewhat greater. Table 2 (columns 6 and 7) also shows that 77% of the CCs in the ll–ts cases were organized as a line of cells (Fig. 4) compared to 47% of the nts events. None of these differences are statistically significant at the 5% level.

Table 3 indicates that 65% of the ll–ts cases occurred on cold frontal days against 47% of the nts cases. The sounding variables, however, exhibit no differences between the ll–ts and nts categories.

Table 4 suggests some differences in severity between the ll–ts and nts cases. The average number of communities reporting water damage was more than

double for the ll–ts MCSs than for nts cases but the nts cases had a somewhat larger average number of communities reporting hail. Table 4 further shows statistically significant differences in maximum hourly rain amount ($p = 0.002$) and the maximum 10-min rain amount ($p = 0.001$). Both were larger for the ll–ts organization. The number of lightning strikes was almost significantly higher for the ll–ts cases ($p = 0.057$), whereas no difference was found for the wind speeds. On the whole, Table 4 shows that the ll–ts organization included the most severe weather as was found by HSD for Oklahoma.

b. Classification of the leading line–trailing stratiform organization

We have found 26 of the 82 MCSs to be of the ll–ts type (32%) and that the ll–ts storms tend to be the most severe. The major springtime rain events in Oklahoma were found by HSD frequently (66%) to exhibit this form of organization. The ll–ts structure is also a characteristic structure of tropical convective systems (e.g., Hamilton and Archbold 1945; Zipser 1969, 1977; Houze 1977; Leary and Houze 1979; Houze and Betts 1981; Barnes et al. 1983; Houze and Rappaport 1984; Gamache and Houze 1985; Houze and Wei 1987; Chong et al. 1987; Drosdowsky and Holland 1987). It therefore seems important to investigate this category of storm in more detail.

To facilitate comparison to the HSD study of Oklahoma storms, we have adopted a methodology similar to theirs. They compared the structure of the radar echoes in each observed case qualitatively to an idealized model of the radar echo structure of a highly organized ll–ts case. They used ten specific characteristics, and decided subjectively if the radar echo in a real case matched the ideal case for each characteristic. One point was assigned to each characteristic. Thus, a perfect match between observed and ideal case had a score of 10. We use the same 10-point system to rate the ll–ts cases in this study. However, we have made some refinements to the technique by trying to associate point values less than 1 with specific ranges of values or patterns, as shown in Fig. 18.

The 10 basic characteristics of ll–ts organization used by HSD include 7 to define the degree of similarity to an ideal leading line and 3 for similarity to an ideal trailing stratiform area (see Fig. 18 and Table 5). Further, they rated the symmetry or asymmetry of the leading line, with respect to the cells it contains and to the location of the trailing stratiform region. Following HSD, the 10 characteristics were scored with 1 point if a particular feature was present and −1 if it was absent. Half points (+0.5, −0.5) were given if the features showed a partial structure, as indicated conceptually in Fig. 18. Information for the 26 ll–ts events was recorded in the same format as in HSD (Table 5), and two scores were computed. Here, C (classifiability) is the sum of the numbers in columns D–J and L–N; this score is listed in column O. It represents the degree that the storm is classifiable, that is the degree to which it exhibits ll–ts structure. A value of C of 5–10 was considered to be "strongly" classifiable by HSD, a value between 0 and 5 "moderately" classifiable, and a value less than or equal to 0 "weakly" classifiable. The second score S (symmetry) is the sum of the data in columns P and Q; this score is shown in column R. It is a number between +2 and −2, which represents the extent to which the MCS exhibits a "symmetric" or "asymmetric" form of ll–ts structure.

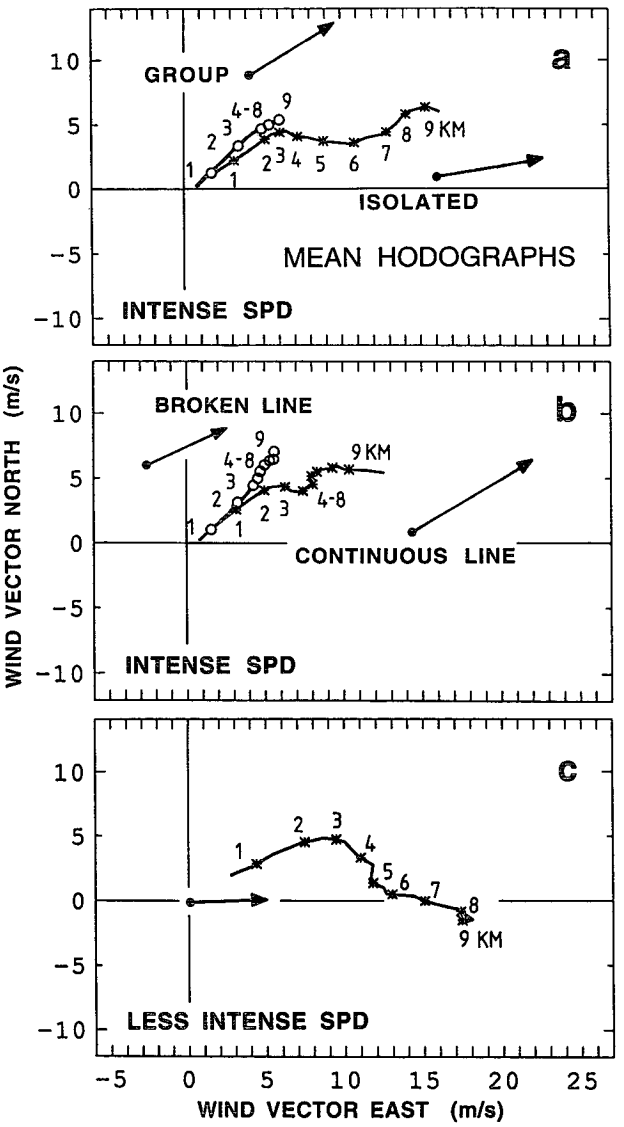

FIG. 14. Mean hodographs for the four intense SPD categories (isolated, group, broken, and continuous line) (a) and (b), and in (c) for the less intense SPDs. For each category the mean storm movement vector is indicated by an arrow.

TABLE 4. Same as Table 2 except for mesoscale precipitation system (MPS) characteristics derived from severe weather reports and surface mesonet variables. Numbers in parentheses are the total number of cases for the subsets restricted to cases with a minimum of either 5 or 20 communities reporting damage.

Column	1	2	3	4	5	6	7	8
				Intense				Less intense
Variables	All	Isolated	Group	Broken line	Cont. line	ll–ts	nts	All
Number of cases	82	22	17	29	14	26	17	12
Water damage reports								
All MPS	7	4.3	6.2	8.1	10.1	11.3	4.9	17.9
MPS min. 5 communities	15.9 (34)	14.8 (6)	18.8 (5)	14.7 (15)	17.3 (8)	16.5 (17)	12. 8 (6)	
Hail damage reports								
All MPS	46.7	27.9[a]	48.1	62.2	42.6	50.8	63.5	
MPS min. 20 communities	60.6 (61)	48.2 (11)[a]	57.9 (14)	71 (25)	52.6 (11)	57.5 (23)	79.5 (13)	
Mesonet								
Max.h.rain (mm h^{-1})	16.2	11.5[b]	13.9[c]	18.5	22	23.1[d]	14.3	9.3
Max.10rain [mm (10 min)$^{-1}$]	8.4	6.4[c]	7.3	9.1	11.4	11.7[d]	6.9	3.4
Max.windgust (m s^{-1})	18.2	16.3[a]	16.4	19.5	20.6	20	19.7	16.3
Max.h.speed (m s^{-1})	6.6	5.8[a]	5.9	7.3	7.1	7.4	7	1.3
Max.h.lightning (h^{-1})	10.7	5.2[e]	10.9	13.2	13.7	15.6	9.9	8.3

[a] sign. less than broken line
[b] sign. less than broken and cont. line
[c] sign. less than cont. line
[d] sign. larger than nts
[e] sign. less than other categories
(in brackets: number of available cases)

Table 5 contains five columns not included by HSD, to give some additional information. Column B contains a "T" or "D." Here T means the stratiform part seemed to trail behind the line for a sufficiently long period that it was not obviously created by a decaying CC behind a new mature line structure. If a decaying CC was clearly responsible for the trailing part, then a letter D was recorded. Either process may produce a trailing stratiform region, and both processes may work together (Houze 1993, chapter 6). Column C shows the time when the leading line was judged to be in the mature stage, column K the time when the stratiform part reached its maximum size. In 13 cases, both mature stages (line and stratiform) were evident at the same time. For 12 MCSs, this time varied from −40 to +30 min for the stratiform time relative to the time when the leading line was scored. One exception of +100 min was found for a stationary MCS on 9 September 1988, the line of which was at its maximum extent when it formed, and the stratiform part grew very slowly from the stationary line. That case is described in more detail in Schiesser et al. (1992). Column S shows the number of communities reporting water damage and T the number of communities reporting hail damage.

The 10 basic characteristics used by HSD to classify the Oklahoma storms were only partly present in the Swiss systems (see Table 5). The most common features were "leading line solid" (20 out of 26), "orientation of line" (22), and the "secondary maximum" of reflectivity in the stratiform area (23). Approximately half of the cases had an "arclike shape" of the leading line (12), a rapid "speed" of line-movement (14), or a "strong radar reflectivity gradient" at the leading edge (14). In only 8 out of 26 ll–ts cases did the stratiform region reach a size of at least 10 000 km^2. The "serrated edge," the "elongated cells," and the "notch" feature were seldom evident.

Strongly classifiable MCSs were not found in Switzerland during the 5-yr period. Of the 12 moderately classifiable MCSs (reaching a score C between 0 and 5 in column O), 5 were organized in the symmetric configuration ($S = 2$), 4 were intermediate ($S = 0$), and 3 were asymmetric ($S = -2$). Figure 19 shows 6 MCSs that were moderately classifiable at the time the scoring of the leading line was done. Continuous-line cases are shown in Figs. 19a, 19e, and 19f, while broken-line cases are represented in Figs. 19b–d. Of these 6 examples, 2 are symmetric, 2 intermediate, and 2 asymmetric in organization. The examples in Fig. 19 may be compared to the examples of moderately classifiable Oklahoma MCSs shown in Fig. 13 of HSD.

A weakly classifiable score ($C = -5$ to 0) was calculated for 13 MCSs. Another case was judged −7, which means almost no resemblance to ll–ts organization. Of these 14 events, 6 were symmetric, 3 inter-

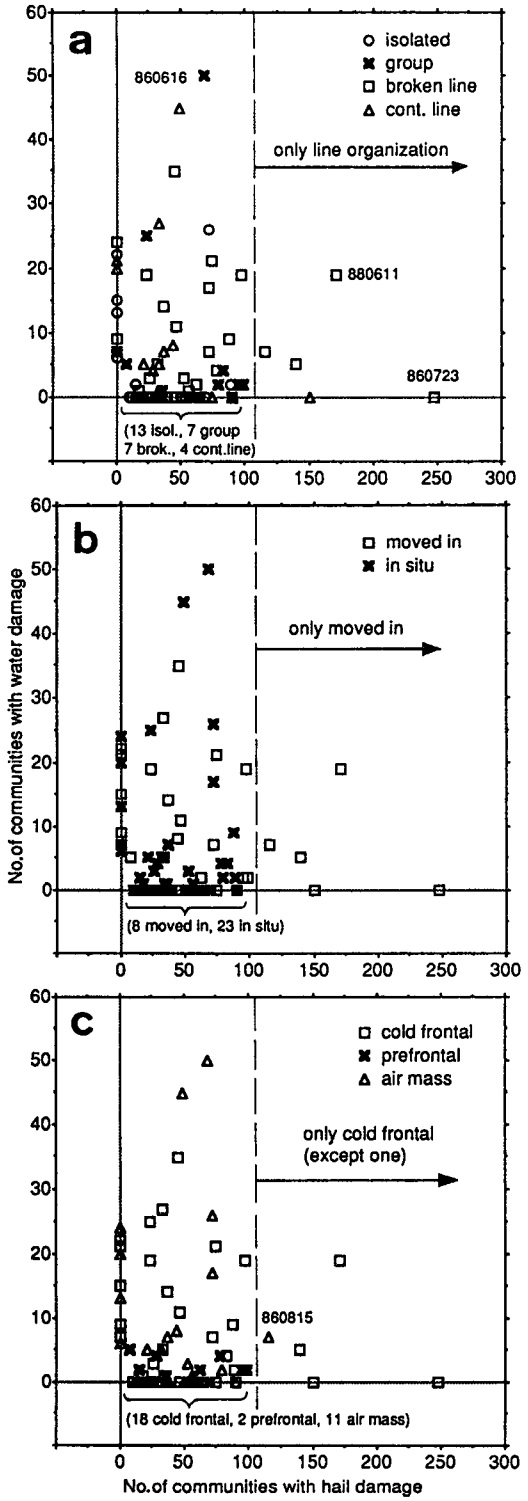

FIG. 15. Scatterplot of the mesoscale convective systems (MCS) with highest number of reporting communities on each day categorized as a severe precipitation day (SPD). The number of communities reporting hail damage vs number reporting water damage is plotted in (a) according to the four categories of mesoscale organization, in (b) according to the origin of the MCS, and in (c) according to the synoptic weather type.

mediate, and 5 asymmetric. Examples of weakly classifiable ll–ts organization are given in Fig. 20. In general, these MCSs were much smaller than the moderately classifiable cases, except for the MCS of 1 July 1987 (Fig. 20a), which was a huge squall line moving into the study area from the northwest, which was quite unusual for the origin of severe convective storms in Switzerland (Fig. 9).

The environmental conditions for the moderately and weakly classifiable ll–ts organization can be summarized as follows: The temperature soundings were similar, and CAPE was only slightly lower in case of the weakly classifiable MCSs but much lower than for the Oklahoma storm environment. In the case of moderate MCSs, Oklahoma storms had a mean CAPE of 1313 compared to 819 J kg^{-1} for the Swiss storms. There was a difference between the convective temperatures, which must reach 29°C to release convection in case of the moderately classifiable MCSs as compared to 24°C for the weaker cases. A significant difference was found between the two hodographs. The hodographs of the moderately classifiable cases were similar to the ones representing the continuous-line category in Fig. 14b. The hodographs representing the weakly classifiable MCSs were similar to those of the broken-line MCSs in Fig. 14b. But both hodographs showed far weaker wind speeds and shear than the hodographs of the corresponding Oklahoma samples (Figs. 17 and 18 of HSD).

To investigate whether a particular type of ll–ts organization favors any type of severe weather, the severe

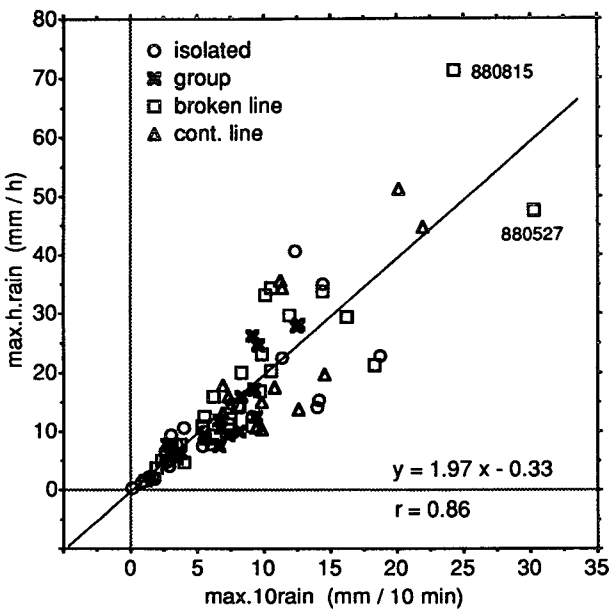

FIG. 16. Scatterplot of maximum amount of rainfall in a 10-min period (max.10rain) vs maximum amount of rainfall during 1 h (max.h.rain). The four categories of radar echo structure are marked with different symbols. A regression line is shown.

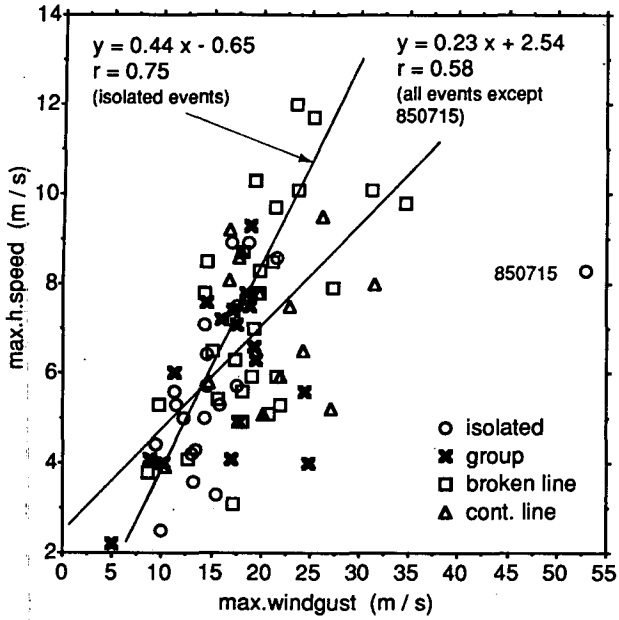

FIG. 17. Scatterplot of maximum wind gust vs maximum average hourly wind speed. The four categories of radar echo structure are marked with different symbols. Two relations are indicated by regression lines, one for all cases and the other for isolated mesoscale convective systems only (both regressions computed without the outlier of 15 July 1985).

weather data for the ll–ts category (column 6, Table 4) are subdivided and averaged by degree of classifiability and symmetry. The results are listed in Table 6 (which can be compared with Table 6 of HSD). Because of the small sample size, the results in Table 6 must be viewed with caution. [Interestingly, the sample size in this study (26 cases) is similar to that of HSD (28 cases)].

For all six measures of severe weather, the moderately classifiable MCSs generally have a somewhat higher value than the weakly classifiable MCSs for all degrees of symmetry as well when all degrees are grouped together, except for the hail parameter, which is higher in case of the intermediate and asymmetric weakly classifiable organizations. The moderately classifiable cases, however, have nearly twice as many instances of water damage and many more lightning counts. HSD found that, overall, flooding was favored in the Oklahoma storms by symmetric structure, but that result was dominated by the highly classifiable cases, which seldom occur in Switzerland. Within the moderately and weakly classifiable structures, like those in Switzerland, the Oklahoma storms also have more flooding associated with asymmetric MCSs (Table 6 of HSD).

Table 6 suggests that asymmetry does not strongly favor hail in Switzerland, as HSD found to be the case in Oklahoma (their Table 6). To investigate this result further, Fig. 21 displays the number of communities reporting hail damage against score C. The shape of the symbols indicate the symmetry score S (column R in Table 5). In addition, the symbols of the cases with at least 10 water damage reporting communities are filled in with black, and the events in which the stratiform region clearly formed by decaying convective cells are marked with the letter D (cases labeled D in column B of Table 5). The five cases with the lowest C scores belong to this category. No strong pattern emerges from this figure. The four cases with 90 or more hail reports are all of the symmetric type in contrast to the Oklahoma storms studied by HSD, in which hail was strongly favored by the asymmetric structure.

Differences between this study and that of HSD may be the result of sampling. However, the differences and relative absence of characteristic features may also be attributed to the fact that topography and low-level wind shear of the two regions are vastly different. The mountains of Switzerland must constrain the mesoscale structures that can occur. Probably the absence of strongly classifiable ll–ts structure in Switzerland is related to the topography not allowing this high degree of organization to develop. The mountainous terrain to the northwest and south of the study area in northern Switzerland evidently disrupts airflow patterns and prevents storms from developing to the same high degree of organization as can occur over the plains of Oklahoma. The MCSs have neither the time nor space they need to reach full development in the Swiss Mittelland. Low-level moist air blows unrestricted into the Oklahoma plains from the Gulf of Mexico. In contrast, the Alps block moisture from blowing into Switzerland from the Mediterranean Sea. Whatever organization MCSs already have on arrival in the Swiss Mittelland becomes quickly disturbed by effects of the terrain. Further the CAPE and wind shear is far weaker in the Swiss environment than in the plains of Oklahoma (Table 9 in HSD). However, if the storm is large enough—for example, the stratiform part reaches a size of 10 000 km^2, enough of the basic features become pronounced that the score C can be in the range 0.5–4.5, which is in the "moderately classifiable" range of HSD.

A further difference in the two studies lies in the selection procedure for cases to be included. The HSD study selected all major rain events in Oklahoma, whether they produced damaging weather or not. Our study selects only cases producing hail or water damage in Switzerland. In a preliminary study of the Swiss cases, Schiesser and Houze (1991) used a selection criterion more similar to the Oklahoma study. They considered seven cases of widespread intense rainfall (not necessarily damaging) in the study area. For this small sample, they found the hail producers to be more associated with asymmetric MCS structure, in agreement with the HSD findings. Only two of those seven cases are in-

Characteristics / Scoring	Leading Line Shape Arc-like	Leading Line Solid	Leading Line Orientation	Leading Line Speed	Leading Line Strong Refl. Gradient
1			SW-NE SSW-NNE S-N	≥12m/s	
0.5			NNW-SSE NW-SE	≥10-12m/s	
-0.5			WSW-ENE WNW-ESE	≥8-10m/s	
-1			W-E	<8m/s	
Characteristics / Scoring	**Leading Line Edge Serrated**	**Leading Line Cells Elongated 45-90°to line**	**Strat. Region Size**	**Strat. Region Notch**	**Strat. Region Secondary Maximum**
1		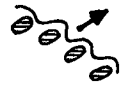	≥ 10'000km2		10 mm/h some area
0.5			≥ 7'500-10'000km2		3 mm/h larger area
-0.5			≥ 5'000-7'500km2	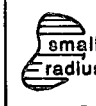	3 mm/h smaller area
-1			< 5000km2	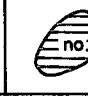	1 mm/h area only

FIG. 18. Pictorial guideline for scoring of the 10 basic characteristics of the idealized leading line–trailing stratiform type of mesoscale convective system.

cluded in the present dataset (17 August 1987; 7 August 1989).

6. Conclusions

The mesoscale structures of the severe mesoscale precipitation systems (MPS), occurring over a 5-yr period in northern Switzerland, have been classified by analyzing the composite radar images of two operational weather radars. Days on which at least 5 communities (out of about 2400) reported water damage and/or at least 20 communities reported hail damage were selected for study, and they were called severe precipitation days (SPD). Of 120 days fulfilling the SPD criteria, 94 had a complete set of daily radar information. If several MPSs (areas enclosed by a radar contour of 25 dBZ reaching a dimension of at least 100 km) occurred during an SPD, only the one with most communities reporting damage was included in the study in order to reduce the available set of MPSs to a manageable size. The 94 SPD days were further subdivided into intense and less intense days. To qualify as intense, one radar image during an SPD had to contain an echo of intensity of at least 47 dBZ. There were 82 intense and 12 less intense SPDs, respectively. The internal radar structures of the 12 less intense cases were not investigated. The 82 MPSs in intense SPDs were referred to as mesoscale convective systems (MCS), and their structures have been examined in detail.

The structure of an MCS was characterized by its internal arrangement of cell complexes (CC) and stratiform precipitation. A CC was defined as a closed echo contour of 40 dBZ surrounding one or more echo maxima of at least 47 dBZ. Four categories of organization were recognized: isolated CC, group, and either a broken or continuous line of CCs. Some MCS were purely convective at the mature stage, whereas others exhib-

TABLE 5. Scoring of mesoscale convective systems with leading line–trailing stratiform type of mesoscale organization. See sections 3 and 5 for further explanation.

A MPS Designator	B ll–ts trailing/ decay	C Time leading line (UTC)	D Lead. line shape arclike	E Lead. line solid	F Lead. line orient.	G Lead. line speed	H Lead. line strong refl. grad.	I Lead. line edge serr.	J Lead. line cells elong. 45°–90° to line	K Time strat. region (UTC)	L Strat. region size	M Strat. region notch	N Strat. region sec. max.	O Lead. line/trail. strat. score *C*	P Lead. line conv. not biased	Q Strat. region location centered	R Symm. vs asymm. score *S*	S Damage MPS water	T Damage MPS hail
85.06.06	T	1650	0.5	−1	−0.5	1	0.5	−1	−1	1700	0.5	−1	0.5	−1.5	1	1	2	0	24
85.07.04	T	1640	1	1	0.5	1	1	−1	−1	1640	1	−0.5	1	4	1	−1	0	27	33
86.05.23	T	1540	−1	1	−0.5	1	1	0.5	−1	1550	−0.5	−1	1	0.5	1	1	2	21	0
86.05.27	D	1730	−0.5	0.5	−0.5	−1	−0.5	−0.5	0.5	1730	−1	−1	0.5	−3.5	−1	−1	−2	19	23
86.06.20	D	1740	1	1	0.5	−0.5	1	−0.5	−1	1800	−0.5	−1	0.5	0.5	−1	−1	−2	45	49
86.07.03	D	1250	−1	1	0.5	−0.5	−1	−1	−1	1250	−1	−0.5	1	−3.5	1	1	2	3	25
86.08.15	T	1720	0.5	0.5	1	1	1	−0.5	−1	1710	1	−0.5	1	4	1	1	2	7	115
86.08.18	T	1330	−0.5	0.5	1	1	−0.5	0.5	1	1250	1	−1	1	4	1	1	2	11	46
87.07.01	T	1040	−1	−1	−0.5	−0.5	1	−1	−0.5	1050	1	−0.5	0.5	−2.5	1	1	2	19	97
87.07.08	T	1500	−1	−1	1	−1	1	0.5	0.5	1500	−0.5	−1	1	−0.5	1	1	2	9	0
87.08.17	T	1820	0.5	0.5	1	0.5	−1	1	0.5	1820	1	−0.5	1	4.5	−1	−1	−2	14	36
87.09.01	T	1800	1	1	1	1	−1	−0.5	−1	1830	−1	−1	−1	−1.5	1	1	2	0	22
88.05.08	T	2100	−1	0.5	0.5	−1	1	−1	−1	2100	−1	−1	−1	−5	1	−1	0	7	71
88.05.19	D	1430	1	1	0.5	0.5	−1	−1	−1	1430	−1	−1	1	−1	1	−1	0	0	74
88.05.27	D	1630	−1	−1	0.5	−1	−1	−1	−1	1630	−1	−1	0.5	−7	−1	−1	−2	9	87
88.06.11	T	1600	0.5	0.5	0.5	0.5	−1	−1	−1	1600	1	−0.5	1	0.5	1	1	2	19	171
88.06.27	D	1830	−0.5	1	0.5	−1	−1	−1	−1	1830	−1	−1	1	−4	1	1	2	7	36
88.06.29	T	1830	0.5	1	1	−1	−1	−0.5	−1	1900	−0.5	−1	1	−1.5	1	−1	0	5	21
88.08.16	D	1230	1	1	1	0.5	1	−0.5	−1	1230	−1	−0.5	1	2.5	1	−1	0	8	43
88.08.28	D	1850	−1	−1	1	1	1	−0.5	−0.5	1840	0.5	−1	1	0.5	1	−1	0	0	46
88.09.09	T	1640	−0.5	1	1	−1	1	−0.5	−1	1820	1	−0.5	1	1.5	1	−1	0	20	0
89.06.27	T	1900	1	1	1	1	1	−0.5	−0.5	1930	−1	−0.5	1	3.5	1	1	2	0	90
89.07.07	T	2030	1	−1	1	1	−1	−1	−1	2030	−0.5	0.5	−1	−2	−1	−1	−2	2	62
89.07.10	T	1450	−1	1	1	−0.5	1	−1	−1	1440	−0.5	−0.5	1	−0.5	−1	−1	−2	35	45
89.08.07	D	1710	−1	1	1	1	1	−0.5	−1	1710	1	−0.5	1	3	−1	−1	−2	4	28
89.08.22	D	1510	−1	1	1	−1	−1	−0.5	−1	1530	−1	−1	1	−3.5	−1	−1	−2	4	78

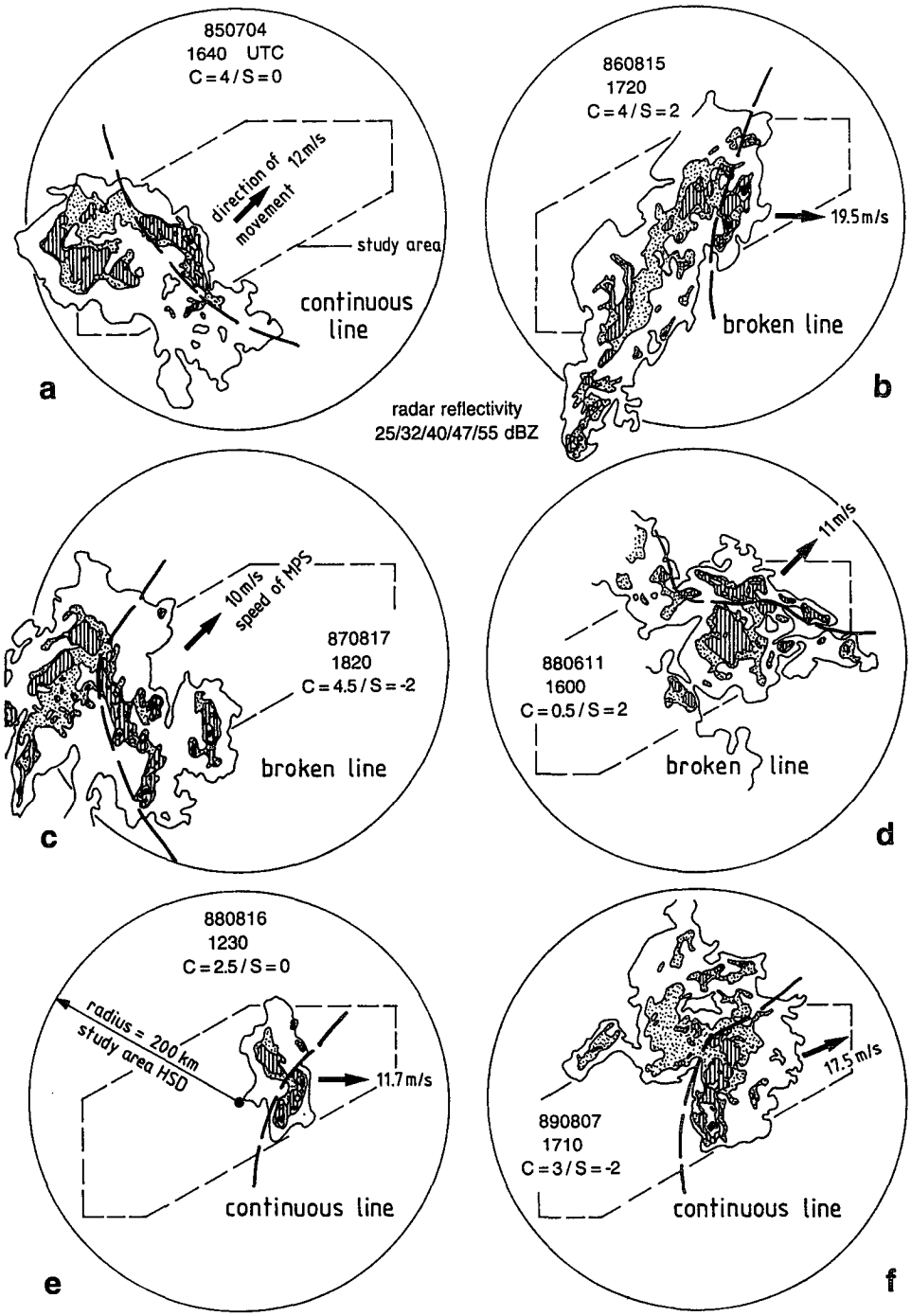

FIG. 19. As in Fig. 6 except for six examples of mesoscale convective systems (MCS) with moderately classifiable leading line–trailing stratiform structure. Bold dashed line separates the MCS into its leading line and trailing stratiform regions. The date, time, *C* score, and *S* score are shown for each case.

ited convective cells juxtaposed with a stratiform precipitation area, which was usually behind the moving convection—a so-called trailing stratiform region—or, more rarely, ahead of the convection. The stratiform region could often be seen to evolve from a decaying convective area.

Each of the categories of mesoscale organization have been examined with respect to radar echo char-

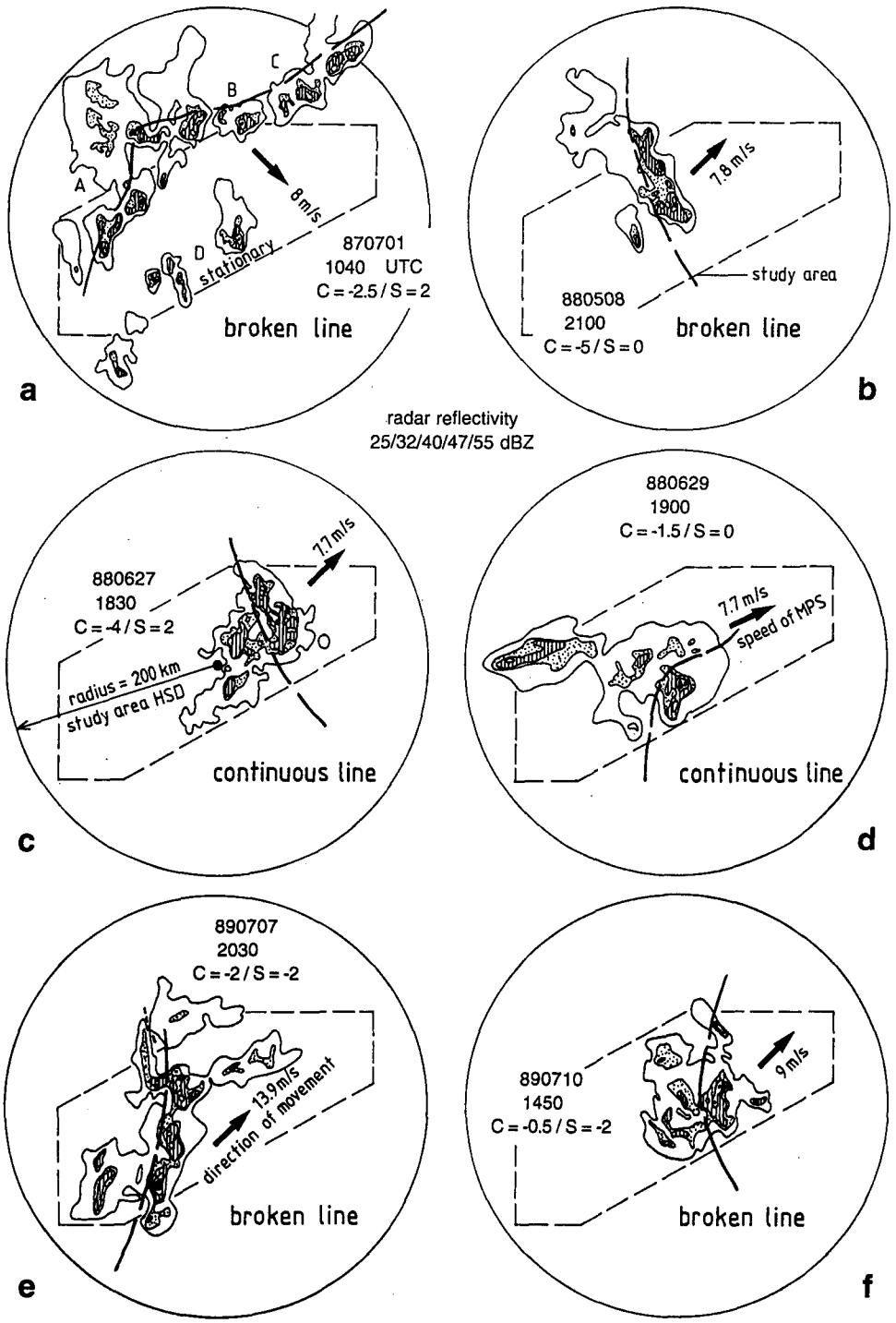

FIG. 20. As in Fig. 19 except for six weakly classifiable MCSs.

acteristics, weather and sounding data, reports of hail and water damage, and surface mesonet observations.

The broken- and continuous-line MCSs tended to move into the region from the west. The isolated and group MCSs tended to form over the low Jura Mountains in the northwest part of the study area. MCSs tended to reach their most severe stage over the low rolling terrain of the central Mittelland, between the Jura Mountains and the foothills of the Alps to the south.

TABLE 6. Summary of characteristics of mesoscale convective systems with leading line–trailing stratiform type of mesoscale organization.

Degree of organization	Degree of symmetry: Symmetric	Intermediate	Asymmetric	All types
Number of cases				
Moderately classifiable	5	4	3	12
Weakly classifiable	6	3	5	14
All classifiable	11	7	8	26
Water damage reporting communities				
Moderately classifiable	11.6	13.8	21	14.7
Weakly classifiable	6.3	4	13.8	8.5
All classifiable	8.7	9.6	16.5	11.3
Hail damage reporting communities				
Moderately classifiable	84.4	30.5	37.7	54.8
Weakly classifiable	34	55	59	47.5
All classifiable	56.9	41.1	51	50.8
Maximum hourly rainfall (mm h^{-1})				
Moderately classifiable	26.4	28.9	28.2	27.7
Weakly classifiable	17.9	13.6	23.8	19.1
All classifiable	21.8	22.3	25.5	23.1
Maximum 10-min rainfall [mm (10 min)$^{-1}$]				
Moderately classifiable	10.5	12.4	15.7	12.4
Weakly classifiable	10.1	8.7	13.9	11.1
All classifiable	10.3	10.8	14.6	11.7
Maximum gust speed (m s^{-1})				
Moderately classifiable	24.4	19	20.2	21.5
Weakly classifiable	17.4	17.5	20.9	18.7
All classifiable	20.6	18.4	20.7	20
Maximum hourly number of lightning				
Moderately classifiable	14.8	26.8	18	19.6
Weakly classifiable	10.2	10.3	15.8	12.2
All classifiable	12.3	19.7	16.6	15.6

The greatest differences were found between the systems with an isolated CC and the significantly larger systems (group, broken-, and continuous-line structure). The mean wind speed between 3- and 10-km altitude and the vertical wind shear (speed) were considerably greater for the isolated category, while the convective temperature, the 0°C level, the cloud base, the equilibrium level, as well as the CAPE were less than in the other categories, whereas the Showalter Index was higher than for the line categories.

The isolated MCSs had lower numbers of damage reports than other MCS structures. Because of their smaller size, isolated MCSs affected fewer communities. However, the isolated MCSs also had lower maximum hourly and 10-min rain amounts, hourly wind speed, maximum gust, and number of lightning events. The group category ranged between the isolated and the two types of line structure. The line structure cases exhibited the highest number of water and hail damage reports and the largest values of the wind, rain, and lightning variables.

Most (80%) of the isolated events developed in situ, as compared to about half of the line formations. The MCSs with highest number of hail damage reports as well as the mixed (water and hail) cases moved into the study area. The two cases with most water damage grew in situ. About half of the SPDs were days on which a cold front passed through Switzerland. On 80% of those days, the front arrived during the second half of the particular day (when conditions are diurnally most favorable for the development of severe storms, especially, if a maritime-tropical air mass lies ahead of the cold front). The most severe hail cases were observed on frontal days, whereas the two most severe events of water damage occurred on airmass days.

Altogether, 43 of the 82 MCS had line structure, of these 26 (i.e., 32% of all MCS) had "leading line–trailing stratiform" (ll–ts) structure. The ll–ts cases produced more severe water damage than lines with no trailing stratiform structure. They also had greater

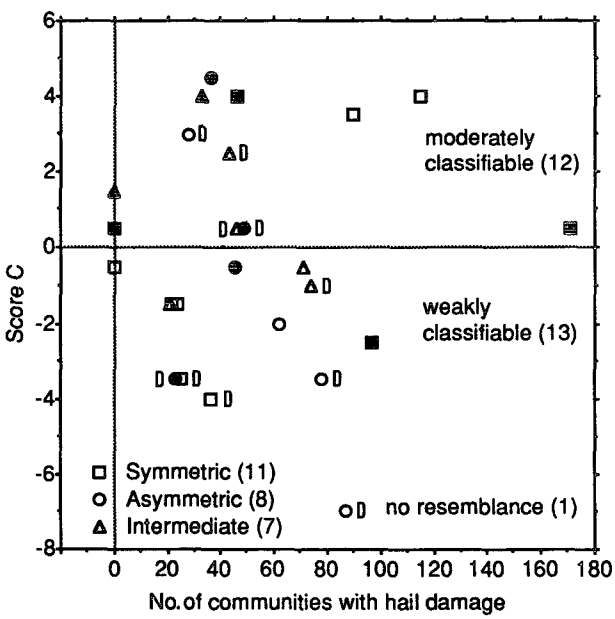

FIG. 21. Scatterplot of number of communities reporting hail vs score *C* for cases of leading line–trailing stratiform organization. The events are stratified according to symmetry score *S* (symbols indicated in the figure). Cases with water damage reported by at least 10 communities are in black. The cases for which the trailing stratiform type of organization is clearly produced by decaying convective cells are marked with the letter D.

hourly and 10-min rain rates and produced more lightning.

Classification of the ll–ts organization after the scheme of HSD, which was developed for major rain events in Oklahoma, showed that similar but more weakly organized ll–ts structures occur in Switzerland. The strongly classifiable ll–ts cases of HSD—that is, nearly ideal examples of leading line–trailing stratiform radar echo pattern—were not seen in our 5-yr sample of data from Switzerland. The mountainous terrain to the northwest and south of the study area in northern Switzerland evidently prevented storms from developing such a high degree of organization. Further, the CAPE and wind shear were far weaker in the Swiss air masses than in the United States. Nonetheless, moderately and weakly classifiable MCSs can develop in the Swiss environment. These results indicate that similar storm organizing processes are at work in the Swiss and Oklahoma storms and suggest that were it not for the complex topography and a somewhat more stable environment, the Swiss storms would also attain the ideal leading line–trailing-stratiform structure embodied in the highly classifiable structure. This hypothesis could be tested in a numerical model.

The moderately classifiable MCSs with ll–ts structure tended to produce somewhat more hail and water damage reports, heavier rain, stronger winds, and more lightning than the weakly classifiable cases. However, the differences were less than a factor of 2. Water damage and lightning were slightly more frequent in asymmetric than in symmetric ll–ts cases, but again differences were less than a factor of 2 on average. Hail was about equally frequent in symmetric and asymmetric MCSs, a result somewhat different from that obtained by HSD, who found a strong preference for hail in asymmetric cases.

Our radar echo classification scheme and documented characteristics of severe mesoscale precipitation systems responsible for hail and water damage in Switzerland provide useful basic information for forecasting, modeling, and climatology of severe storms affecting Switzerland. It will facilitate comparison of future or historical severe MPSs with the investigated ensemble and will provide the basis for an expanded climatology of severe MPSs. In the extension of this work, it should not be necessary to rely on the hail and water damage reports. A more objective severe-storm criterion would be based on the radar data alone. Since at least one hail cell or a cell-producing intense rain is responsible for any instance of hail or water damage, a peak radar reflectivity criterion, which has been used to identify the severe hail cells, could be used in future for the selection of the MCSs. This criterion identifies a cell as a region of at least 47 dBZ with a maximum intensity of at least 55 dBZ observed for a minimum of 30 min. In the category of the ll–ts organization, such cells were present in 21 out of 26 MCSs, while another three cases nearly fulfilled the criterion (20 min). The two cases that did not fulfill the selected criterion were purely rain events. Thus, the radar criterion appears to be a reliable indicator of severe hail events. With this criterion as a basis, a complete climatology of the MCSs for the years 1983 up to now can be established. Data from the SMA radars have been archived for that length of time. In addition Doppler radar measurements are now being made regularly at ETH in Zürich, and a monitoring of such hail cells satisfying the above mentioned criterion was introduced in 1992 in the framework of NFP31 (Radar Meteorology Group 1993, radar data available). The extended climatology will provide a context into which these new data can be evaluated.

Acknowledgments. This research was supported by the National Science Foundation of Switzerland under Grant 4031-033526 within the National Research Program 31 "Climatic Changes and Natural Disaster," the U.S. National Science Foundation under Grant ATM-9101653, and the Swiss Hail Insurance Company. Gerhard Röthlisberger of the Federal Institute of Forestry Research (WSL) permitted us to use his collection of water damage data. Dr. Bradley Smull provided generally helpful comments and advice.

APPENDIX

Variables Used to Describe Mesoscale Precipitation Systems

The following information has been recorded for each of the 94 mesoscale precipitation systems in this study. These data are the basis for the figures and tables presented in this study. The full dataset is published in a report of the Radar Meteorology Group (1994) and is available on request (Institute of Atmospheric Science, ETH-Hönggerberg, 8093 Zürich, Switzerland). For the abbreviations see text.

a. General information from synoptic data, radar, and damage reports

Date: 880712—Year, month, day.

SPD-water: Total number of communities reporting damage by water per day (minimum of 5 reports).

SPD-hail: Total number of communities with damage by hail per day (minimum of 20 reports).

Weather 1: Occurrence or nonoccurrence of intense precipitation during an SPD. *Intense* is defined as an SPD showing at least one radar echo of 47 dBZ. Nonoccurrence is recorded as *less intense.*

Weather 2: Indication of the occurrence of a *warm frontal, cold frontal, prefrontal* (cold front passage next day, intermediate stage between cold frontal and air mass) or of an *airmass* day (no front next day) according to records of the SMA.

Time of front: Time of occurrence of front within Switzerland. Categories are *first* [during first half of day, 2300–1100 UTC (0000–1200 LST)], *second*

[during second half of day, 1100–2300 UTC (1200–2400 LST)]. Data from records of SMA.

Air mass noon: The type of air mass over Switzerland at 1100 UTC (1200 LST). Categories are *arctic, maritime polar, continental polar, maritime tropical, continental tropical.* Data from records of SMA.

No. MPS: Total number of distinguishable mesoscale precipitation systems (MPS) in study area during a particular SPD day. An MPS showing intense precipitation is called mesoscale convective system (MCS).

MPS: Ordinal number of the most severe system of the SPD. All further variables are determined for this MPS.

MPS water: Number of communities with water damage associated with the most severe MPS of the day.

MPS hail: As above but for hail damage.

Max. dimension (km): The maximum horizontal extent during the lifetime of an MPS of the 25-dBZ radar contour outlining the stratiform precipitation region.

Only study area: This parameter refers to the maximum size of the 25-dBZ contour. *Yes* is recorded, if the contour is only within the study area, *no,* if the contour extends outside the study area.

Mode origin/end: Indicates whether the particular MPS developed in situ or moved into the study area (=origin) and decayed in situ or moved out of the study area (=end): i/i—in situ/in situ; i/m—in situ/moved out; m/i—moved in/in situ; m/m—moved in/moved out.

Loc. of orig.: The location of origin of the first 25-dBZ echo is given for eight particular regions within the study area (according to climatic and topographic regions in use by the SMA) and an additional four directions if the systems are large and move along a broad front toward the study area. The locations are (Fig. 2 and 3a) JW—Jura west; JE—Jura east; MW—Mittelland west; MZ—Mittelland zentral (central); ME—Mittelland east; AW—Alps west; AZ—Alps zentral (central); AE—Alps east; and the four main wind directions W, S, E and N.

Merger: "No" is the indication if there is no merger (interaction) between MPS or smaller features, and "yes" if there is such a merger.

Dir. mov. (°): Direction of movement of the whole MPS. The direction is given in steps of 22.5°. If the direction is indicated as 0 (zero), then the system had no discernible movement. The movement of the radar echoes was determined by viewing the radar film in motion picture mode and tracking identifiable features.

Speed mov. (m s^{-1}): The speed of the movement of a system is determined by viewing the radar film in motion picture mode and tracking identifiable features over a time period about 2 h or so.

Start time (UTC): The time when the first in situ development was noted or when the 25-dBZ radar contour crosses the border of the study area. See also day start.

Day start: A system can start on the *same* day or on a day *before* the SPD. If the day start is indicated as "before," then the start time will be declared for the day before.

Lifetime (h): The lifetime gives the time span within which the system was present in the study area. If the system moved out, the time was taken until the 25-dBZ radar contour completely crossed the border of the study area.

Conv. org.: Convective organization of the MPS having intense precipitation. The four types of organization are *isolated, group, broken line,* and *continuous line* (see text for details). If there is no indication of intense precipitation then the system is called *less intense* (as defined in weather 1).

Length of line (km): The maximum length of the broken or continuous line of radar echo of at least 40 dBZ.

Strat. area: An indication whether a stratiform area is present at the same time a convective complex is observed: none—no stratiform, ahead—stratiform area ahead of convective region, and trailing—stratiform present behind convective region.

No. CC: Number of cell complexes during the lifetime of a system within the study area. The complexes are observable during a time span of 30–60 min and are readily distinguishable from each other.

Time CC (UTC): The time of the largest cell complex of the system at the instant when the complex appears to be most severe.

Location: The location of the largest cell complex at "time CC." The localities are the same as for "Loc. of orig." but without the four main wind directions (Fig. 3a).

Org. CC: The small-scale internal organization of the most severe complex is indicated to be either *one cell,* or a *line of cells* (Fig. 4).

Dim. CC (km): The dimension of the cell complex expressed as the maximum horizontal extent of the isolated 40-dBZ radar contour in any single direction.

b. *Sounding information*

Date. S: Date of sounding: year, month, day.

Sond (UTC): Time of sounding.

Winddir850 (°): Wind direction at 850 hPa.

Speed850 (m s^{-1}): Wind speed at 850 hPa.

Winddir700 (°): Wind direction at 700 hPa.

Speed700 (m s^{-1}): Wind speed at 700 hPa.

Winddir500 (°): Wind direction at 500 hPa.

Speed500 (m s^{-1}): Wind speed at 500 hPa.

M.Winddir3–10 (°): Mean wind direction between 3 and 10 km.

M.Windspeed3–10 (m s^{-1}): Mean wind speed between 3 and 10 km.

Shear2.5–6 (°): Direction of shear between 2.5 and 6 km.

Shear2.5–6 (m s^{-1}): Speed of shear between 2.5 and 6 km.

Shear0–6 (°): Direction of shear but between ground level and 6 km.

Shear0–6 (m s^{-1}): Speed of shear but between ground level and 6 km.

Conv.temp (°C): Temperature which has to be reached at ground level to make the layer below the level of free convection adiabatic.

0°C level (m): Freezing level.

CCL (m): Height of convective condensation level (as defined by Petterssen 1956a).

Showalter index (°C): Modified Showalter index, the difference between the temperature of a parcel lifted from the CCL level (instead surface level) and the environment temperature at 500 hPa (Showalter 1953).

Eq.level (m): Height at which temperature of a lifted parcel becomes equal to the environmental temperature.

CAPE (J kg^{-1}): Convective available potential energy (as defined by Weisman and Klemp 1982).

c. *Mesonet data*

Anetzall: Number of available stations in or around the damage area of the particular MPS.

max.h.rain (mm h^{-1}): Maximum amount of rainfall in 1h during the lifetime of the system.

max.10rain [mm (10 min)$^{-1}$]: Maximum amount of rainfall in a 10-min period during the lifetime of the system.

max.windgust (m s^{-1}): Maximum wind gust during the lifetime of the system.

max.h.speed (m s^{-1}): Maximum hourly wind speed during the lifetime of the system.

max.h.lightning (h^{-1}): Maximum number of lightning strikes per hour.

REFERENCES

Barnes, G. M., E. J. Zipser, D. Jorgensen, and F. D. Marks Jr., 1983: Mesoscale and convective structures of a hurricane rainband. *J. Atmos. Sci.*, **40,** 2125–2137.

Browning, K. A., 1990: Organization and internal structure of synoptic and mesoscale precipitation systems in midlatitudes. *Radar in Meteorology,* D. Atlas, Ed., Amer. Meteor. Soc., 433–460.

Chong, M., P. Amayenc, G. Scialom, and J. Testud, 1987: A tropical squall line observed during the COPT 81 experiment in west Africa. Part I: Kinematic structure inferred from dual-Doppler radar data. *Mon. Wea. Rev.*, **115,** 670–694.

Donaldson, R. J., Jr., 1958: Analysis of severe convective storms observed by radar. *J. Meteor.*, **15,** 44–50.

Douglas, R. H., and W. Hitschfeld, 1959: Patterns of hailstorms in Alberta. *Quart. J. Roy. Meteor. Soc.*, **85,** 105–119.

Drosdowsky, W., and G. J. Holland, 1987: North Australian cloud lines. *Mon. Wea. Rev.*, **115,** 2645–2659.

Federer, B., A. Waldvogel, W. Schmid, H. H. Schiesser, F. Hampel, M. Schweingruber, W. Stahel, J. Bader, J. F. Mezeix, N. Doras, G. d'Aubigny, G. DerMegreditchian, and D. Vento, 1986: Main results of Grossversuch IV. *J. Climate Appl. Meteor.*, **25,** 917–957.

Feldman, D. S., Jr., J. Gagnon, R. Hofmann, and J. Simpson, 1987: *StatView II, The solution for Data Analysis and Presentation Graphics.* Abacus Concept Inc., 278 pp.

Gamache, J. F., and R. A. Houze Jr., 1985: Further analysis of the composite wind and thermodynamic structure of the 12 September GATE squall line. *Mon. Wea. Rev.*, **113,** 1241–1259.

Hagen, M., 1992: On the appearance of a cold front with a narrow rainband in the vicinity of the Alps. *Meteor. Atmos. Phys.*, **48,** 231–248.

Hamilton, R. A., and J. W. Archbold, 1945: Meteorology of Nigeria and adjacent territory. *Quart. J. Roy. Meteor. Soc,* **71,** 231–262.

Houze, R. A., Jr., 1977: Structure and dynamics of a tropical squall line system. *Mon. Wea. Rev.*, **105,** 1540–1567.

——, 1981: Structures of atmospheric precipitation systems—A global survey. *Radio Sci.*, **16,** 671–689.

——, 1993: *Cloud Dynamics.* Academic Press, 573 pp.

——, and A. K. Betts, 1981: Convection in GATE. Rev. Geophys. Space Phys., **19,** 541–576.

——, and P. V. Hobbs, 1982: Organization and structure of precipitating cloud systems. *Adv. Geophys.*, **24,** 225–315.

——, and E. N. Rappaport, 1984: Air motions and precipitation structure of an early summer squall line over the eastern tropical Atlantic. *J. Atmos. Sci.*, **41,** 553–574.

——, and T. Wei, 1987: The GATE squall line of 9–10 August 1974. *Adv. Atmos. Sci.*, **4,** 85–92.

——, B. F. Smull, and P. Dodge, 1990: Mesoscale organization of springtime rainstorms in Oklahoma. *Mon. Wea. Rev.*, **118,** 613–654.

——, W. Schmid, R. G. Fovell, and H. H. Schiesser, 1993: Hailstorms in Switzerland: Left movers, right movers, and false hooks. *Mon. Wea. Rev.*, **121,** 3345–3370.

Huntrieser, H., H. H. Schiesser, and A. Waldvogel, 1994: The synoptic and mesoscale environment of severe convective activity in Switzerland. *Proc. Int. Symp. on the Life Cycle of Extratropical Cyclones,* Bergen, Norway, Norweg. Geophys. Soc. and Amer. Meteor. Soc., Vol. 3, 101–106.

Joss, J., and G. Kappenberger, 1984: Quantitative measurement of precipitation with radar in an alpine country. Preprints, *22d Conf. on Radar Meteorology,* Zürich, Switzerland, Amer. Meteor. Soc., 270–275.

——, and A. Waldvogel, 1990: Precipitation measurement and hydrology. *Radar in Meteorology,* D. Atlas, Ed., Amer. Meteor. Soc., 577–606.

Leary, C. A., and R. A. Houze Jr., 1979: Melting and evaporation of hydrometeors in precipitation from anvil clouds of deep tropical convection. *J. Atmos. Sci.*, **36,** 669–679.

Meischner, P. F., V. N. Bringi, D. Heimann, and H. Höller, 1991: A squall line in southern Germany: Kinematics and precipitation formation as deduced by advanced polarimetric and Doppler radar measurements. *Mon. Wea. Rev.*, **119,** 678–701.

Petterssen, S., 1956a: *Weather Analysis and Forecasting.* Vol. 1. McGraw-Hill, 428 pp.

——, 1956b: *Weather Analysis and Forecasting.* Vol. 2. McGraw-Hill, 266 pp.

Radar Meteorology Group, 1993: Monitoring of severe hail storms in Switzerland 1992. LAPETH-30, 163 pp. [Available from Atmospheric Science, ETH, CH-8093 Zürich, Switzerland.]

——, 1994: Monitoring of severe hail storms in Switzerland 1993. LAPETH-31, 200 pp. [Available from Atmospheric Science, ETH, CH-8093 Zürich, Switzerland.]

Schiesser, H. H., 1990: Hailfall: The relationship between radar measurement and crop damage. *Atmos. Res.*, **25,** 559–582.

——, and R. A. Houze Jr., 1991: Mesoscale organization of precipitation systems in Switzerland. Preprints, *25th Int. Conf. on Radar Meteorology,* Paris, France, Amer. Meteor. Soc., 509–512.

——, and S. Willemse, 1992: About the origin, extent and frequency of severe hailstorms in Switzerland north of the alpine ridge. Preprints, *22d Int. Conf. on Alpine Meteorology,* Toulouse, France, Société Météorolgique de France, 403–407.

——, R. A. Houze Jr, and A. Waldvogel, 1992: Mesoscale organization of precipitation systems causing severe damage by in-

tense or long-lasting rain in Switzerland. *Int. Symp. on Interpraevent,* Vol. 1, Bern, Switzerland, 71–82.

Schmid, W., H. H. Schiesser, and A. Waldvogel, 1992: The kinetic energy of hailfalls. Part IV: Patterns of hailpad and radar data. *J. Appl. Meteor.,* **31,** 1165–1178.

Showalter, A. K., 1953: A stability index for thunderstorm forecasting. *Bull. Amer. Meteor. Soc.,* **34,** 250–252.

Waldvogel, A., and W. Schmid, 1982: The kinetic energy of hailfalls. Part III: Sampling errors inferred from radar data. *J. Appl. Meteor.,* **21,** 1228–1238.

——, B. Federer, W. Schmid, and J. F. Mezeix, 1978: The kinetic energy of hailfalls. Part II: Radar and hailpads. *J. Appl. Meteor.,* **17,** 1680–1693.

Weisman, M. L., and J. B. Klemp, 1982: The dependence of numerically simulated convective storms on wind shear and buoyancy. *Mon. Wea. Rev.,* **110,** 504–520.

——, and ——, 1984: The structure and classification of numerically simulated convective storms in directionally varying wind shears. *Mon. Wea. Rev.,* **112,** 2479–2498.

Zeller, J., and G. Röthlisberger, 1988: Unwetterschäden in der Schweiz im Jahre 1987. *Wasser, Energie, Luft,* **80,** 29–42.

Zipser, E. J., 1969: The role of organized unsaturated convective downdrafts in the structure and rapid decay of an equatorial disturbance. *J. Appl. Meteor.,* **8,** 799–814.

——, 1977: Mesoscale and convective-scale downdrafts as distinct components of squall line circulation. *Mon. Wea. Rev.,* **105,** 1568–1589.